Bay-wide abundance estimates and recruitment strength of native and non-native oysters (*Ostrea lurida*, *Crassostrea gigas*) in San Diego Bay, CA

Final Report

Prepared by: Bryce Perog, Ty Frantz, Chelsea Bowers, Marah Wolfe, and Dr. Danielle Zacherl

California State University Fullerton

December 2020

INTRODUCTION

Estuaries and bays provide important habitat for a wide array of fish, bird, and invertebrate species. Urbanization, resource use, and commercialization have resulted in drastic decreases in the abundance of native estuarine species through habitat reduction and modifications to the natural hydrology (Lotze, 2006; Van Dyke & Wasson, 2005). As the effects of climate change become more pronounced, shoreline armoring in the U.S. has increased in frequency to protect the thousands of structures located near the shoreline (NOAA Fisheries, 2020). The introduction of breakwaters, jetties, and seawalls can fragment or eliminate natural habitats (Bulleri & Chapman, 2010; Goodsell et al., 2007) and accelerate erosion (Gittman et al., 2015). Reductions in native species through anthropogenic modifications can also impact critical ecosystem services, leaving these habitats at risk for poor water quality and invasions by introduced species (Lotze et al., 2006, Wells et al., 2019).

Non-indigenous species (NIS) have established populations in areas outside of their native distribution, typically as a result of deliberate or accidental human activity. NIS may become invasive if they have adverse economic or ecological consequences, including the reduction in native species richness or abundance associated with the establishment of invasive sessile invertebrates (Blum et al., 2007). Estuaries are highly invaded relative to the open coast (Ruiz et al., 1997), and the introduction of aforementioned anthropogenic structures can favor the settlement of NIS (Airoldi et al., 2015; Bulleri & Chapman, 2010; Tyrrell & Byers, 2007), including the non-indigenous Pacific oyster, *Crassostrea gigas* (Scanes et al., 2016). Long-term monitoring of NIS is necessary to identify trends between their distribution and long-term factors including climate change and habitat transformation (Pyšek et al., 2020).

Understanding the relative abundance of both native species and NIS of interest can provide a clearer picture of the state of their populations that can be tracked through time. Density is the number of individuals per unit area, while abundance is the overall number of individuals in an area. Density can be used to extrapolate the abundance of individuals in an area, but sites and habitats are highly variable in the number and diversity of animals they can support. Density and abundance estimates can expose areas with low abundances that can be targeted for restoration. Abundances can be estimated through various methods, including line transects, mark-recapture, and statistical modeling. Abundance estimate methods are well-established for mobile species including harbor porpoises (Hiby & Lovell, 1998), lake fish larvae (McKenna Jr. & Johnson, 2009), endangered vaquitas (Jaramillo-Legorreta et al., 1999), rare blue whales (Williams et al., 2011), and economically important blue crabs (Zohar et al., 2008). Remote sensing via satellite imagery has be used to opportunistically estimate abundances of congregating species (Moxley et al., 2017), marine macro-debris on the shoreline (Kataoka et al., 2018), and intertidal algae and subtidal kelp beds (Mora-Soto et al., 2020). Plant abundance estimates have been investigated by extrapolating the percent cover values of woody plants (Cornwell & Ackerly, 2010), and may be applied to sessile animals. The habitats for the organisms targeted are generally homogenized, whereas intertidal habitats are heterogenous. Estuarine intertidal habitat can be highly variable, especially with the increase in shoreline armoring (see example of California counties in Griggs & Patsch, 2019) and site-specific

differences of intertidal species densities (Zacherl, unpub. data). Challenges with estimating abundance of organisms in heterogenous environments have been addressed for invasive oyster drills (Buhle & Ruesink, 2009), horseshoe crabs hibernating in winter (Liang et al., 2017), and salamanders (Dodd Jr & Dorazio, 2004), but the estimates have the added complexity of difficulty of detection. Heterogenous environments that yield patchy distributions of intertidal swash-zone species have advised using models instead of extrapolating density measurements (Defeo & Rueda, 2002), however, sessile mussel abundances have also been estimated using randomly-placed quadrats along transect to determine density, which, when multiplied by habitat area, can provide abundance estimates (Bodkin et al., 2018; Pooler & Smith, 2005). Although changes in oyster abundance have been studied over time (Zu Ermgassen et al., 2012; Zu Ermgassen et al., 2016), they used harvest amounts and reef size (when present) as proxies for abundances, and did not quantify commonly-found remnant oysters settled upon habitats other than oyster grounds. If oysters did not exist in high enough densities to form beds or reefs, they were eliminated from consideration. Currently, oysters on the U.S. west coast rarely form high-density oyster grounds, so new methods to estimate their abundances must be explored.

The native Olympia oyster, *Ostrea lurida,* is distributed from British Columbia to Baja California (Polson & Zacherl, 2009). It was historically abundant along its range, and wild *O. lurida* populations were used for aquaculture until their reefs were depleted at which point non-native Pacific oysters imported from Japan were implanted into the estuaries to supplement the industry (Barrett, 1963). In San Diego Bay, native oyster reefs were present but not abundant enough to support harvest by as early as the 1930s due to pollution in the bay (Bonnot, 1935). Today, *C. gigas* are well established throughout the *O. lurida* geographic range (Polson & Zacherl, 2009), including in San Diego Bay (Crooks et al., 2015; Tronske et al., 2018). *C. gigas* may have a facultative (Figures 1 and 2) or detrimental (Buhle & Ruesink, 2009; Krassoi et al., 2008; Trimble et al., 2009) role in *O. lurida* recovery, so it is critical to establish the two species' abundance where their distributions overlap.

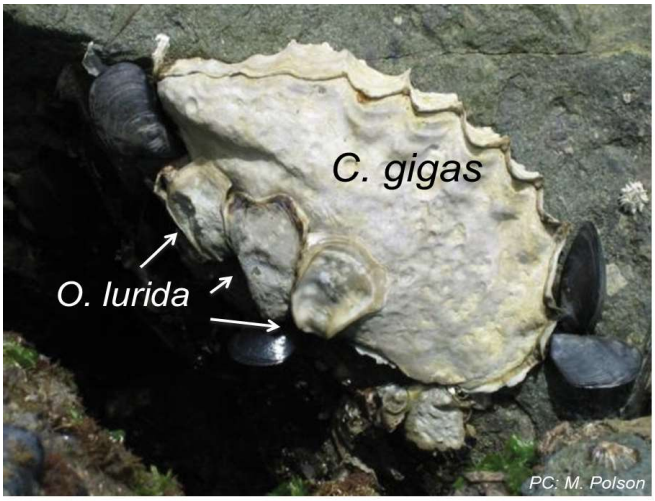

Figure 1. Possible *C. gigas* facultative effect on *O. lurida* recruitment. *M. galloprovincialis* shown growing alongside the oysters.

Figure 2. Sixteen *O. lurida* recruited to one *C. gigas* (center) on recruitment tile deployed at E Street at 0 m MLLW in San Diego Bay, CA during the 2018 recruitment season. Example of possible facultative effect of *C. gigas* on *O. lurida* recruitment. *O. lurida* may recruit in higher abundances to oyster shell compared to introduced hard habitat.

The Bay mussel, *Mytilus galloprovincialis*, is another non-native bivalve that is established on the west coast of North America (Fofonoff et al., 2018). Its native range is the Mediterranean, but its invasive range is largely unknown partly because *M. galloprovincialis* is a morphologically cryptic species in a species complex with four other *Mytilus sp*. (Fofonoff et al., 2018). *M. galloprovincialis* was introduced to supplement native *M. trossulus* aquaculture on the west coast of North America, including in Agua Hedionda Lagoon in San Diego County (Shaw, 1997), but its mechanism of spread to other areas in California is largely unknown (Fofonoff et al., 2018). *M. galloprovincialis* was first detected in San Diego in 1987 by molecular analysis (McDonald & Koehn, 1988) and has since hybridized with the native *M. trossulus* (Braby & Somero, 2006). *M. galloprovincialis* can cause reduced growth and survival of native mussels (Shinen & Morgan, 2009). Recent mussel surveys have yielded only *M. galloprovincialis* or hybrids in select southern Californian estuaries (Garcia, Walter, and Zacherl, unpublished data).

O. lurida, *C. gigas*, and *M. galloprovincialis* co-occur within estuarine intertidal habitat. Their adult densities overlap but are partly separated by tidal elevation, where *C. gigas* is found at higher tidal elevations, *O. lurida* is found at lower tidal elevations, and *M. galloprovincialis* is found between and among the two oyster species (Figure 3). Bivalves provide important ecosystem services (see review, Padilla, 2010). For example, oysters, as foundation species, increase ecosystem productivity (Peterson & Heck Jr., 1999), provide water filtration, improve water quality, and enhance available habitat (Coen et al., 2007). Oysters sequester carbon when

they deposit carbon-rich seston into the sediment and facilitate the expansion of other carbon sinks (Fodrie et al., 2017) and contribute to bioremediation (Dalrymple & Carmichael, 2015).

Figure 3. Example zonation of the three species of interest on a seawall in Alamitos Bay, CA in 2013. *C. gigas* is at the highest elevation, *M. galloprovincialis* is in the middle, and *O. lurida* is within and below the band of mussels.

San Diego Bay has the highest percentage of hard armor on the shoreline among counties in California (Griggs & Patsch, 2019). The San Diego Bay Integrated Natural Resources Management Plan has reviewed the negative environmental impacts to the bay from armored shorelines and have goals to reduce their impact and improve estuarine ecosystem health. Of the intertidal habitat in the bay, 74% has been armored since 1859 (U.S. Department of the Navy, Naval Facilities Engineering Command Southwest & Port of San Diego, 2013). Though the habitat in the intertidal has changed dramatically, the artificial hard habitat is still utilized by intertidal organisms, including by oysters and mussels. The Port of San Diego is interested in establishing baseline abundance estimates of native *O. lurida*, non-indigenous *C. gigas*, and non-indigenous *M. galloprovincialis* in San Diego Bay and monitoring them over time to inform aquaculture and blue technology opportunities in the bay.

STUDY OBJECTIVES

We aim to estimate bay-wide abundances of oyster and mussel species by conducting field studies in a variety of locations around the bay with varying habitat types to assay intertidal oyster and mussel abundance and density. This field survey potentially is the first of a recurring set of sampling throughout San Diego Bay. In addition, we will deploy recruitment tiles to understand the current reproductive capacity of both oyster species in the bay.

Study Questions

This final report will address the following general questions:

1. What are the densities of native Olympia oysters, *Ostrea lurida* and non-native Pacific oysters, *Crassostrea gigas* at sites throughout San Diego Bay and how have the densities changed over time?[1]
2. What is the total estimated bay-wide abundance of both oyster species?
3. What is the strength of oyster recruitment during the summer 2020 oyster reproductive season and how does it compare to previous years?

STUDY DESIGN & METHODS

Field Surveys

In 2020 we surveyed *Ostrea lurida* and *Crassostrea gigas* density, percent cover, bay-wide abundance, and substratum availability at 11 sites spanning the perimeter of the Bay. These sites were selected based on accessibility, diversity of habitat types, and were distributed throughout the entire bay (Figure 4). When possible, we sampled multiple sites with the same substratum availability to generate average densities on particular habitat types including pier piling, pipe, chain-link fence, seawalls, cobble fields, riprap, and mud and sand habitats. All sites were sampled during the summer of 2020 between the months of June and July.

At each site, we surveyed the tidal range from the waterline of the respective lower low tide to the highest live oyster. At sites with cobble, riprap, and mud and sand, 2-3 50 m transects were laid out to divide the habitat into equal sections to capture the density of oysters across the available tidal range. Sites with pier piling, pipe, chain-link fence, or seawall habitat were surveyed using a single 10-18 m transect placed above the visible oyster zone. X and y-values were randomized for the placement of the 0.5-m length x 0.5-m length (0.25 m^2) quadrats (n=38-45 per site, n=6-45 within each habitat type). For sites with pier piling, pipe, chain-link fence, or seawall habitat, we reduced the quadrat size to 0.5-m length x 0.15-m length (0.075 m^2) quadrats to constrain each individual quadrat to more specific tidal elevations.

[1] Per the contract, bay-wide abundance and density estimates will be calculated for *Mytilus galloprovincialis*, too. We collected data on % cover across all sites and took photo plots at a subset of sites. These data can eventually be converted into density estimates and used to estimate bay-wide abundance for this species. Here, we provide a qualitative assessment of their abundance.

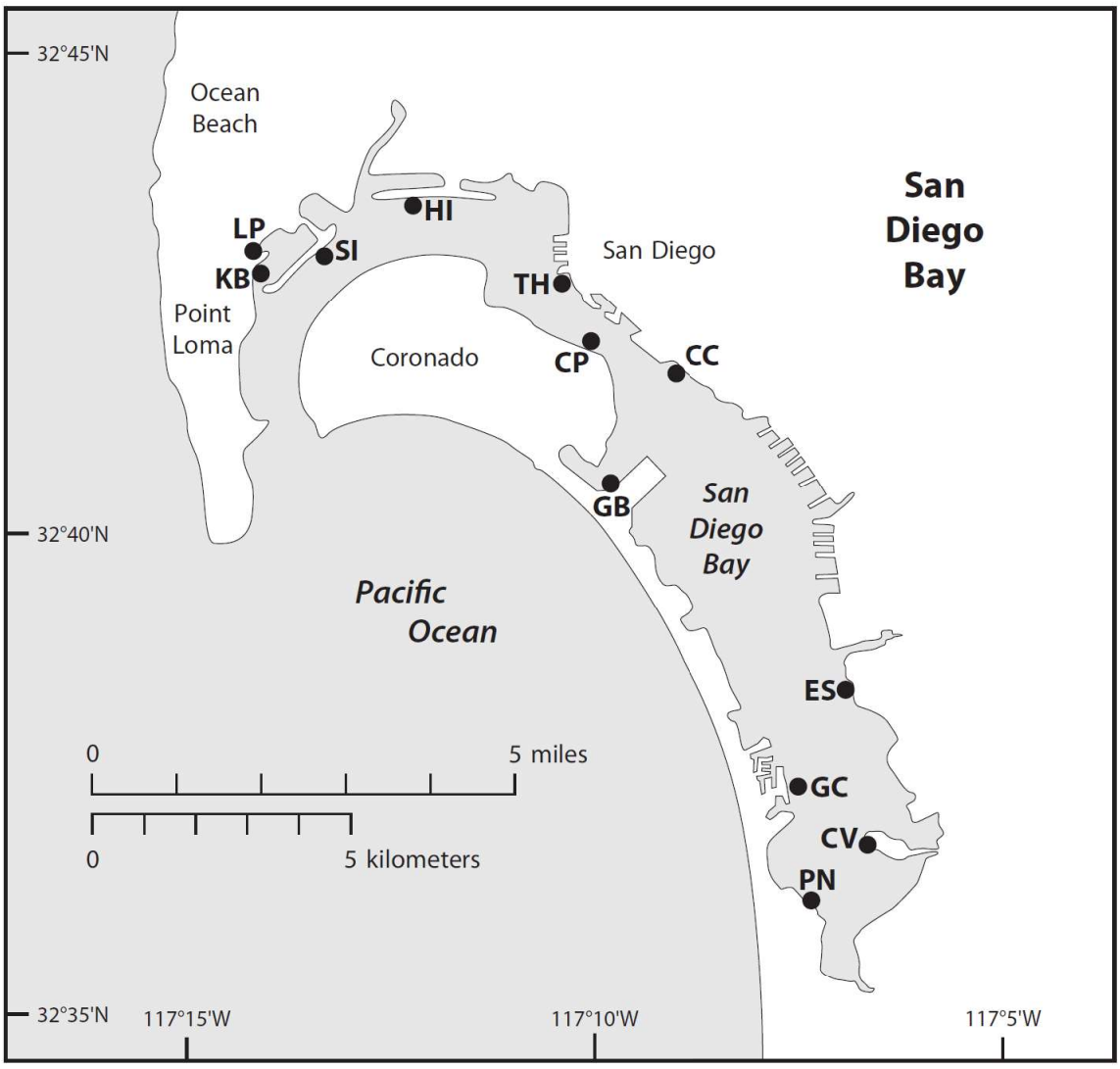

Figure 4. Locations of study sites in San Diego Bay, CA, for field surveys and recruitment tile deployments during 2020.

To determine substratum availability within the habitats we employed a point contact technique, using a gridded 0.25 m^2 quadrat with 21-49 points based on the habitat type. At each point we identified the substratum first encountered with our probe. Alga and eelgrass (*Zostera marina*) points were only counted if the probe hit the holdfast. Otherwise, the alga or eelgrass cover was moved to reveal the substratum beneath. Mobile organisms were removed and the substrate beneath was counted. Hard substrate types encountered included wall, fence, gravel, small rock, medium rock, large rock, boulder, concrete, pier piling, wood, terracotta, rebar, engine, beer bottle, glass, live and dead *O. lurida*, live and dead *C. gigas*, live and dead *Amphibalanus amphitrite*, live *Musculista senhousia*, live *Mytilus galloprovincialis*, live *Phragmatopoma californica*, and live clam. Soft substrates included mud, sand, *Codium fragile*, *Zostrea marina*, *Ulva*, *Chondracanthus canaliculatus,* tunicates, sea anemone, sponge, bryozoan, and air. These data were used to assign each quadrat to a habitat type (Table 1).

Once percent cover was quantified, we replaced the gridded quadrat with an open quadrat to collect oyster density data. Oysters that were at least halfway into the quadrat were identified and counted. We identified all live oysters by external examination of the shell based on presence/absence of shell foliations (*C. gigas*) or by internal identification of the presence/absence of chomata (as in Polson et al., 2009; Raith 2013). The size of the first 25 encountered oysters from each species was recorded by each surveyor across 4 surveyors for a total of 100 oysters per species measured per site at GC, CV and GB. For the remaining sites, we recorded the first 5 oysters encountered per quadrat until we reached 25 measured by each surveyor across 4 surveyors for a total of 100 oysters per species measured per site. Size frequency distribution data were not included in this final report since they were beyond the scope of the contract but are available upon request.

To capture the tidal elevation at each site we used a Laser Mark LM-30 rotary laser by calculating the difference in height from an established watermark at a specific time and using predicted NOAA tidal elevations (Station ID: 9410170). We estimated the tidal elevation for each quadrat (see Table 1 for tidal elevation range for each site).

Oyster density data were converted to per m^2 and then combined with data we generated on bay-wide habitat availability (see below) to estimate bay-wide abundances for both oyster species. We calculated density above and below 0.3 m MLLW within each site on several habitat types including seawall, rip rap, pier pilings, cobble, soft sediment, pipe, and chain-link fence, and then generated average densities across sites per habitat type and tidal elevation. These averages were multiplied by the area (length * width) of each habitat around the perimeter of the bay to generate bay-wide abundance estimates. To incorporate pipe into the perimeter, the width of four pipes were measured and applied to all pipes found in the bay (0.9 m * 37 pipes).

Bay-wide pier piling area was estimated as 1.2 m height * 0.3 m width * 4 sides * # of pier pilings bay-wide. However, for several reasons, we elected to use seawall density data to represent oyster densities on pier piles: 1) we sampled only 7 pier pilings and only at a single site that may not be representative of the bay, 2) we detected an error in our tidal elevation measurements for the pier pilings and confirmed the error using time-stamped images of surveyors working on the pier pilings; sorting out which quadrats to assign to which tidal elevation became problematic, 3) we recorded unusually high *O. lurida* density and unusually low *C. gigas* density on these pier pilings that we were not confident were representative of the bay-wide densities on that habitat, 4) seawall was the next-best proxy for measuring densities on piling directly.

Recruitment study

We assessed recruitment of *O. lurida* and *C. gigas* by deploying concrete tiles as a proxy for available habitat on March 22 and 23, 2020, at four sites, GC, CV, ES, and LP (Figure 4). Smooth concrete tiles were constructed and suspended from PVC pipes modeled after Seale and Zacherl (2009) in vertical and horizontal orientation (Figure 5) at two tidal elevations that reflect the adult distributions of *O. lurida* (0 m MLLW) and *C. gigas* (+0.6 m MLLW; Tronske et al., 2018) (n= 5 tiles per orientation, site and tidal elevation). The PVC pipes were inserted into the mud or sand habitat so that tiles hung approximately 12-15 cm above the ground. In addition to the concrete tiles, we also deployed replicate (n=3) terra cotta tiles in plastic mesh cages at ES to

standardize the recruitment substrate to previous years of collected recruitment data. Tiles deployed at GC were damaged or lost during the study, and thus they are excluded from analyses.

Recruitment tiles were retrieved on October 18, 2020. Tiles were processed first by capturing an image of both sides of every tile (Figure 6 and Appendix A). Then, percent cover of organisms on each tile was assessed using a 50-point gridded quadrat point contact technique on each side of the tile. Substrate types included: concrete tile, terracotta tile, live and dead *O. lurida*, live and dead *C. gigas*, live and dead *Amphibalanus amphitrite*, *Watersipora sp., Bugula sp*., *Styela plicata*, and other tunicates. On both sides of the tiles, live and dead oysters were identified and counted. The maximum length (mm) and width (mm) of all live oysters was measured. Oyster size frequency distribution, oyster mortality, and percent cover data analyses were not included in this final report since they were beyond the scope of the contract but are available upon request.

Figure 5. PVC pipe with suspended concrete tiles at La Playa, San Diego Bay, CA in March 2020.

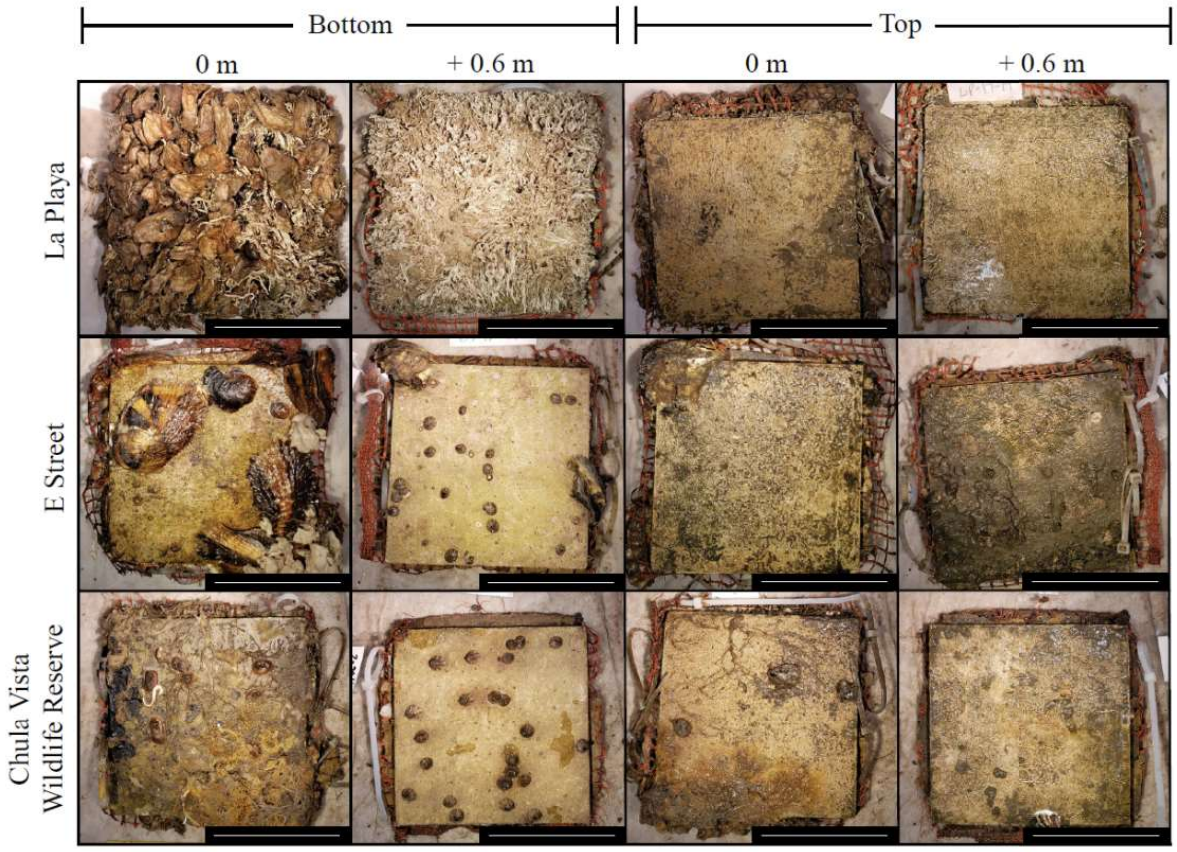

Figure 6. Treatment tiles post-deployment on underside and upper side of tiles orientated horizontally to the water surface. Tiles were deployed at La Playa, E Street, and Chula Vista Wildlife Reserve in San Diego Bay, CA from March to October, 2020. Scale = 10 cm.

Bay-wide Habitat Estimates

We used Google Earth, an open-access database of satellite imagery, to determine substrate type along the entire shoreline of San Diego Bay. A combination of satellite imaging and in-person photos (when available) of the areas were used to identify and measure the distance (in meters) of various habitat types (Figure 7). We characterized cobble as any rock <0.3 m (1 ft) and boulder or rip rap as > 0.3 m (1 ft) in diameter. All satellite photos were captured from 2018 – 2020, per Google Earth. We categorized all substrata into seven types: cobble, fence, pier pile, pipe, boulder (includes rip rap and concrete slabs), seawall, and soft (includes sand and mud). Large areas under structures held by pier pilings where the substrate could not be determined were categorized as "unknown." Pier pilings were counted and are assumed to be underestimated due to the lack of adequate satellite or in-person images provided in Google Earth.

Figure 7. Example of shoreline measured in Google Earth. Satellite imagery was taken at high tide.

Data analysis

Differences in 2020 densities of *O. lurida* and *C. gigas* on the underside of tiles were assessed (separately) as a function of site, tidal elevation, and their interaction using two-way ANOVAS. We also evaluated whether there were differences in density as a function of species and habitat type and their interaction using two-way ANOVAS.

Assessing density changes over time was challenging because of slight variation in the data collection methods (we collected data in 2013 across a limited tidal range centered around 0 m MLLW), but was possible. These data were analyzed by undergraduate scholars participating in the Southern California Ecosystem Research program at CSUF as part of a summer course, BIOL 301, Problems in Environmental Biology under the tutelage of Dr. Zacherl and Dr. Bill Hoese, and their research poster, presented at the Society for the Advancement of Chicanos and Native Americans in Science (SACNAS), a conference of national significance, is included in Appendix B. Differences across years (2013/2014 vs 2017 vs 2020) in *O. lurida and C. gigas* density were each tested using one-way analysis of variance (ANOVA) separately for lower (≤+0.38 m MLLW) and higher tidal elevations (>+0.38 m MLLW).

To assess variation in recruitment across sites in 2020, differences in the number of *O. lurida* and *C. gigas* on the underside of concrete tiles were assessed (separately) as a function of site, tidal elevation, and their interaction using two-way ANOVAS. To understand if the magnitude of recruitment in 2020 was high or low, we examined archived caged recruitment data from E Street previously collected by the Zacherl lab from 2015-2019, combined with 2020 recruitment data. We tested for the effects of year, tidal elevation, and their interaction for each oyster species separately using two-way ANOVAS. Lastly, to understand whether differences in recruitment among sites were maintained from year to year, we again examined archived

recruitment data from 2017-2019 at Glorietta Bay, Grand Caribe and E Street at 0 m MLLW where we tested for the effects of site, year and their interaction on recruitment for each species separately, again by using two-way ANOVAS. For comparisons among vertically and horizontally deployed recruitment tiles from 2020, we analyzed for the effects of treatment (horizontal upper vs. horizontal underside vs. vertical seaward vs. vertical shoreward), tidal elevation, and their interactions on recruitment separately for each species and site.

All data used in the above ANOVAs were square root or log transformed if they did not meet the ANOVA assumption for equal variances. If unequal variances persisted in the data after transformations, then data were rank-transformed and analyzed in non-parametric ANOVAs. If main effects or interaction effects were present, then post-hoc Tukey tests determined the differences among response factors. All ANOVAs were completed in JMP version 14.

RESULTS

Oyster Densities and Tidal Elevation

O. lurida densities across all sites surveyed in 2020 at the lower tidal elevations (<0.3 m) ranged from 0 to 401.0 oysters/m^2 and at the higher tidal elevations (>0.3 m) ranged from 0 oysters/m^2 to 147.5 oysters/m^2 (Table 1). *C. gigas* densities across all sites surveyed in 2020 were generally lower than *O. lurida* at the lower tidal elevations, ranging from 0 oysters/m^2 to 115.7 oysters/m^2, and ranging from 0 oysters/m^2 to 255.1 oysters/m^2 at the higher tidal elevations. *O. lurida* showed trends for higher densities at lower tidal elevations but this effect was site-dependent (2-way ANOVA, 2-way interaction, site*elevation, p<0.0001, Figure 8), and only statistically significant at HI and KB. *C. gigas* displayed an inverse pattern, having significantly higher densities at higher tidal elevations at 5 of 11 sites (2-way ANOVA, 2-way interaction, site*elevation, p<0.0001, Figure 9).

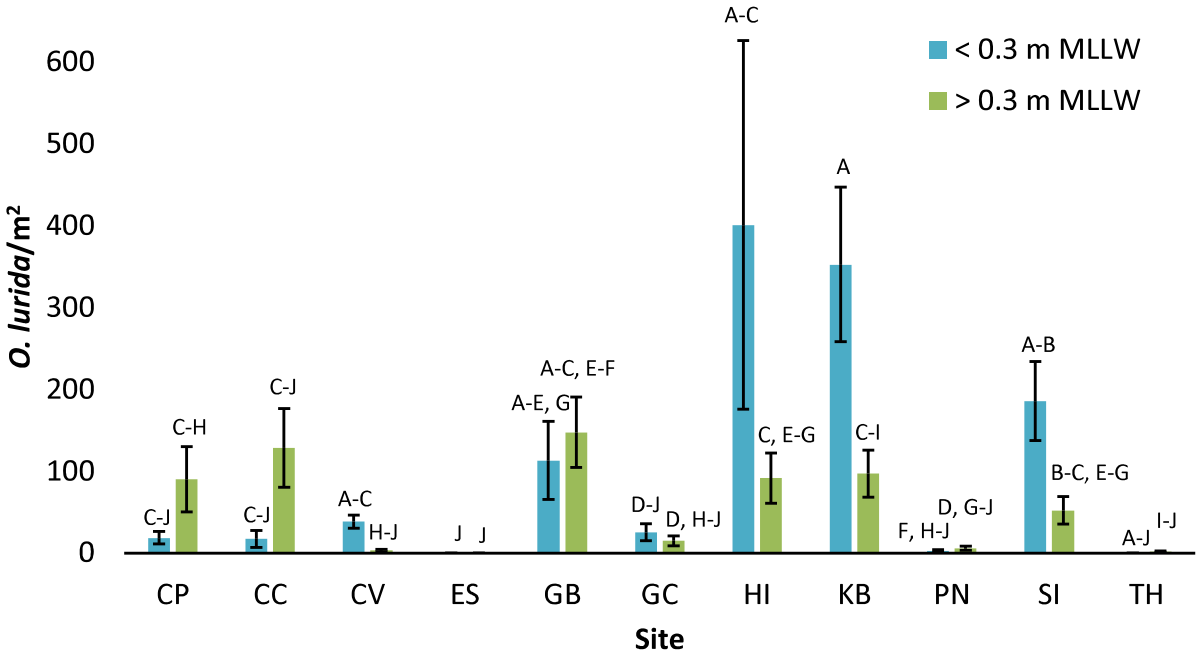

Figure 8. *O. lurida* density across sites in San Diego Bay in 2020 at high and low tidal elevations. Error bars=1 SE. Different letters above bars indicate statistically significant differences based upon post-hoc Tukey HSD tests.

Table 1. Density abundances of *O. lurida* and *C. gigas* from summer surveys in 2020 throughout San Diego Bay, California.

Site	Code	Habitat Type	Date	GPS Coordinates	Tidal Range (m MLLW)	*O. lurida* /m^2 (SE, n)	*C. gigas* /m^2 (SE, n)	*O. lurida* /m^2 <1 ft (SE, n)	*O. lurida* /m^2 >1 ft (SE, n)	*C. gigas* /m^2 <1 ft (SE, n)	*C. gigas* /m^2 >1 ft (SE, n)
Chula Vista											
Wildlife Reserve	CV	Cobble	8-Jun	32.6143,	-0.29 - 1.18	14.2	32.3	38.6	3.2	0.3	46.7
				-117.1138		(3.6, 45)	(6.1, 45)	(8.0, 45)	(1.5. 45)	(0.3, 45)	(7.6, 45)
Grand Caribe	GC	Riprap	9-Jun	32.6263,	-0.04 - 1.19	10.0	61.3	ND	10.0	ND	61.3
				-117.1297		(4.1, 12)	(17.9, 12)	ND	(4.1, 12)	ND	(17.9, 12)
		Seawall	20-Jul	32.6271,	0.19 - 1.26	33.5	87.1	99.0	21.4	0.0	103.2
				-117.1297		(9.9, 45)	(16.1, 45)	(23.6, 7)	(9.8. 38)	(0.0, 7)	(17.9, 38)
		Soft	9-Jun	32.6263,	-0.04 - 1.19	0.7	1.1	0.0	1.7	0.0	2.6
				-117.1297		(0.4, 34)	(0.8, 34)	(0.0, 20)	(0.8, 14)	(0.0, 20)	(2.0, 14)
Glorietta Bay	GB	Fence	10-Jun	32.6751,	0.08 - 1.20	143.5	225.5	113.3	147.6	3.3	255.1
				-117.1674		(38.2, 34)	(31.5, 34)	(47.6, 34)	(43.0, 34)	(3.3, 34)	(31.9, 34)
Pond 11 North	PN	Cobble	23-Jun	32.6027,	-0.26 - 1.01	7.2	18.6	9.0	7.0	0.0	21.3
				-117.1178		(2.6, 31)	(45.4, 31)	(4.4, 4)	(2.9, 27)	(0.0, 4)	(6.1, 27)
		Soft	23-Jun	32.6027,	-0.26 - 1.01	0.3	0.3	0.0	1.0	0.0	1.0
				-117.1178		(0.3, 13)	(0.3, 13)	(0.0, 9)	(1.0, 4)	(0.0, 9)	(1.0. 4)
North	TH	Riprap	24-Jun	32.7118,	0.24 - 1.72	1.9	63.9	0.0	2.0	32.0	64.6
				-117.1746		(0.9, 46)	(7.2, 46)	(0.0, 46)	(0.9. 46)	(0.0, 46)	(7.3, 46)
Kellog Beach	KB	Riprap	22-Jun	32.7114,	-0.11 - 0.89	47.1	87.1	166.2	1.9	136.7	68.3
				-117.2367		(14.3, 40)	(13.7, 40)	(30.5, 11)	(1.3, 29)	(33.5, 11)	(12.8, 29)
		Seawall	25-Jun	32.7119,	0.23 - 0.98	69.6	186.7	746.7	38.8	80.0	191.5
				-117.2365		(32.5, 23)	(20.6, 23)	(0.0, 23)	(11.0, 23)	(0.0, 23)	(20.9, 23)
		Pipe - North	25-Jun	32.7121,	0.15 - 0.89	473.9	280.0	986.7	360.0	20.0	337.8
				-117.2363		(135.0, 11)	(81.6, 11)	(106.7, 11)	(136.3, 11)	(20.0, 11)	(88.7, 11)
		Pipe - South	25-Jun	32.7121,	-0.04 - 0.95	375.8	290.9	1093.3	304.0	226.7	297.3
				-117.2363		(142.0, 11)	(56.5, 11)	(0.0, 11)	(135.4, 11)	(0.0, 11)	(62.1, 11)
		Soft	22-Jun	32.7114,	-0.11 - 0.89	0.0	25.6	0.0	0.0	0.0	32.0
				-117.2367		(0.0,5)	(23.6, 5)	(0.0, 1)	(0.0, 4)	(0.0, 1)	(29.3, 4)
E Street	ES	Mudflat	26-Jun	32.6332,	-0.16 - 1.34	0.0	0.0	0.0	0.0	0.0	0.0
				-117.1076		(0.0, 46)	(0.0, 46)	(0.0, 46)	(0.0, 46)	(0.0, 46)	(0.0, 46)
Harbor Island	HI	Riprap	21-Jul	32.7247,	0.05 - 1.64	126.0	45.0	401.0	91.6	22.0	47.9
Park				-117.2076		(38.7, 36)	(6.2, 36)	(225.3, 36)	(30.8, 36)	(5.8, 36)	(6.8, 36)
Cesar Chavez	CC	Cobble	22-Jul	32.6961,	0.08 - 0.76	12.5	1.3	24.0	1.0	0.5	2.0
Park				-117.1511		(7.3, 16)	(0.6, 16)	(13.7, 8)	(1.0, 8)	(0.5, 8)	(1.1, 8)
		Pier Piling	22-Jul	32.6961,	0.45 - 1.35	317.0	53.3	ND	317.0	ND	53.3
				-117.1511		(140.3, 9)	(17.5, 9)	ND	(140.3, 9)	ND	(17.5, 9)
		Seawall	22-Jul	32.6961,	0.54 - 1.11	101.8	204.8	ND	101.8	ND	204.8
				-117.1511		(45.3, 11)	(51.7, 11)	ND	(45.3, 11)	ND	(51.7, 11)
		Soft	22-Jul	32.6961,	0.08 - 0.76	0.0	0.0	0.0	0.0	0.0	0.0
				-117.1511		(0.0, 6)	(0.0, 6)	(0.0, 3)	(0.0, 3)	(0.0, 3)	(0.0, 3)
Centennial Park	CP	Riprap	23-Jul	32.6998,	-0.11 - 1.15	49.6	94.2	84.0	46.2	4.0	103.2
				-117.1711		(16.6, 22)	(20.0, 22)	(4.0, 2)	(18.1, 20))	(4.0, 2)	(21.0, 20)
		Seawall	23-Jul	32.6998,	0.54 - 1.35	266.7	117.8	ND	266.7	ND	117.8
				-117.1711		(166.6, 6)	(48.1, 6)	ND	(166.6, 6)	ND	(48.1, 6)
		Soft	23-Jul	32.6998,	-0.11 - 1.15	8.9	8.7	10.1	0.0	9.9	0.0
				-117.1711		(4.7, 17)	(8.0, 17)	(5.3, 15)	(0.0. 2)	(9.0, 15)	(0.0, 2)
Shelter Island	SI	Riprap	24-Jul	32.7159,	-0.06 - 1.26	94.8	78.1	185.7	52.4	82.9	75.9
				-117.2230		(21.0, 44)	(10.3, 44)	(48.2, 44)	(16.8, 44)	(15.7, 44)	(13.3, 44)
La Playa	LP	Soft	22-Mar	32.3714,	ND	ND	ND	ND	ND	ND	ND
				-117.2355		ND	ND	ND	ND	ND	ND

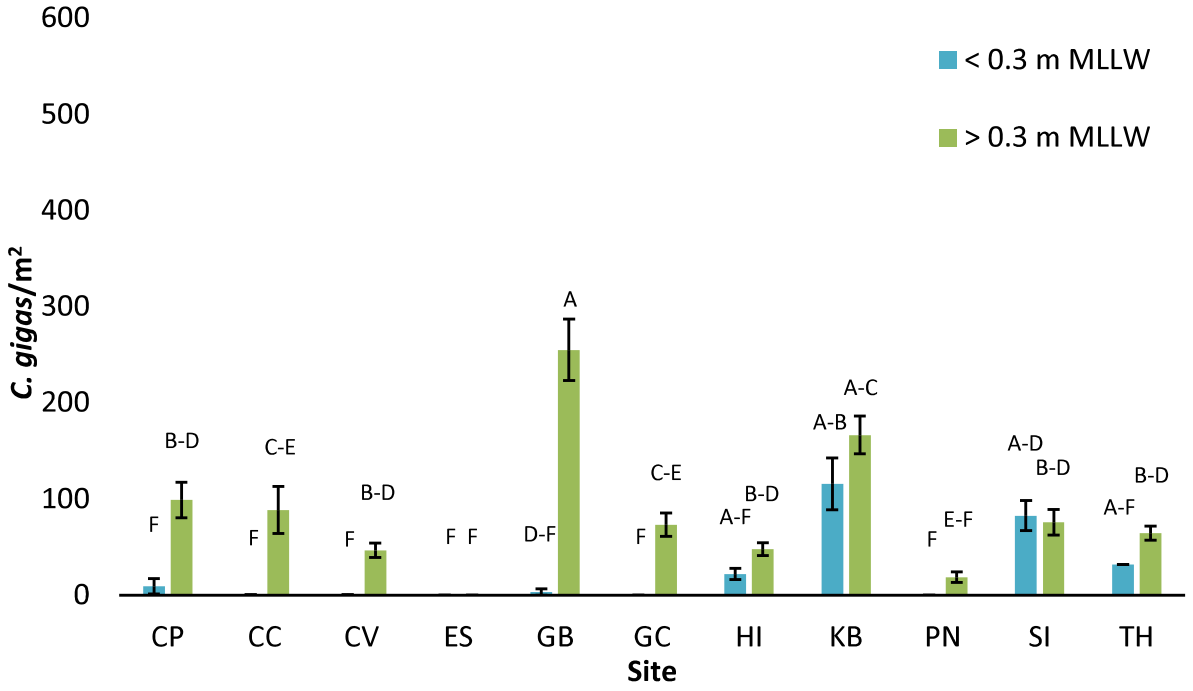

Figure 9. *C. gigas* density across sites in San Diego Bay in 2020 at high and low tidal elevations. Error bars=1 SE. Different letters above bars indicate statistically significant differences based upon post-hoc Tukey HSD tests.

Oyster Densities and Habitat Type

Across all sites, *O. lurida* densities (averaged across all tidal elevations) ranged from 11.6 oysters/m^2 to 473.9 oysters/m^2 on hard substrate. *C. gigas* densities (averaged across all tidal elevations) ranged from 22.3 oysters/m^2 to 290.9 oysters/m^2 on hard substrate. Both species experienced their lowest overall densities in soft sediment, and trended toward their highest densities being represented on a pipe located at Kellogg Beach (Figure 10). Densities of the two species were similar among half of the surveyed habitat types (2-way ANOVA, 2-way interaction, oyster species*habitat type, $p<0.0001$). *O. lurida* densities were higher than *C. gigas* densities on pier pilings and pipe, though none of these differences were statistically significant (post-hoc Tukey comparisons, $p>0.05$ for each listed habitat type). However, *C. gigas* densities were significantly higher than *O. lurida* on seawall, riprap, and fence (Figure 10).

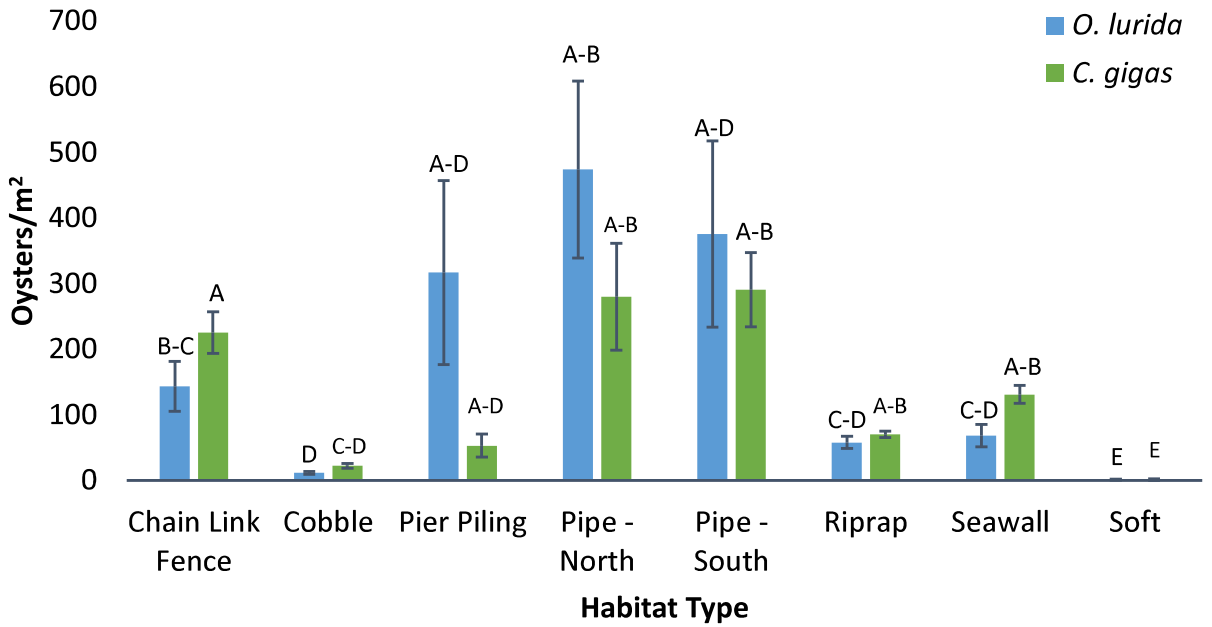

Figure 10. Oyster density across habitat types in San Diego Bay in 2020. Error bars=1 SE. Different letters above bars indicate statistically significant differences based upon post-hoc Tukey HSD tests.

Oyster Density Across Time

O. lurida densities within each site fluctuated across years with no apparent overall trend across sites; at the lower tidal elevation, they declined significantly at CV and GC (ANOVA $p<0.05$ for both sites), and fluctuated at GB (Appendix B, Figure B-5); at the higher tidal elevations, densities were stable at two sites (ANOVA, $P>0.05$), but increased at GB (ANOVA, $p>0.05$). *C. gigas* densities were generally stable at the lower tidal elevation, but increased greater than 5X at two of three sites (ANOVA, $P<0.05$ at CV and GB) at the higher tidal elevation and remained the same at one site (GC) where their density was already high (Appendix B, Figure B-5).

Mussel Density

While we did not quantify mussel density in our open quadrats, density was exceedingly low. *M. galloprovincialis* averaged <0.1% cover on substrata across all sites. The highest *M. galloprovincialis* cover was at Kellogg Beach where they accounted for 5.4% of the cover on habitats at that site (Figure 11), and 94% of the point contact data recording this mussel species across all sites were taken at Kellogg Beach.

Figure 11. *M. galloprovincialis* found at Kellogg Beach, San Diego Bay, CA in July 2020.

Perimeter and Abundance Estimates

Visual surveys using Google Earth revealed that the perimeter of San Diego Bay is comprised mostly of hard substrata that may facilitate oyster recruitment (80.7%, Table 2, Figure 12). Approximately 78.4% of this is made up of human introduced substrate, including riprap and seawalls upon which *C. gigas* densities were higher (Figure 10). Both oyster species were present on each type of hard substrate but at exceedingly low densities on the soft substrate that comprised 18.9% of the bay perimeter. Due to limitations in Google Earth, we could not identify the habitat on ~1.6% of the total bay perimeter. Visual estimates of pier pilings from docks, piers, and other structures revealed an estimated 63,768 pier pilings which provides additional available habitat for both oyster species and *M. galloprovincialis*. Pier pilings varied in size and material, but limitations in Google Earth prevented further categorization. Pipes and chain link fence jutting into the bay added additional oyster habitat to the perimeter of the bay (746 m), while boat launches and outfalls do not provide habitat for oysters (254 m, or <0.01% of San Diego Bay perimeter). While tracing the perimeter of the bay, a possible oyster reef was found in Harbor Island (32.727515°N, 117.194366°W, Figure 13).

The estimated bay-wide abundance for *O. lurida* is 34,318,947, about 1.3 times more than *C. gigas* at 26,014,313 oysters (Table 2). Both species are most commonly found on rip rap, with 54% of *O. lurida* and 46% of *C. gigas* found on this habitat, which is the most common habitat in the bay.

Table 2. Total perimeter (m), percentage of total perimeter, *O. lurida* and *C. gigas* abundances (# of individuals) and % of habitat sampled by the field surveyors in June-July, 2020 for shoreline habitats around San Diego Bay, CA. The "Other" category is combined habitats that comprise 2% of total habitat, including pipe, boat launch, outfall, and unknown.

Habitat type	Perimeter (m)	% of Perimeter	*O. lurida* Abundance	*C. gigas* Abundance	% of Habitat Sampled
Rip rap	41,764	42.2%	18,426,989	11,934,938	0.75%
Seawall	30,307	30.6%	2,900,035	3,516,397	0.53%
Soft	18,727	18.9%	154,030	437,752	1.78%
Cobble	5,550	5.6%	585,575	631,670	2.90%
Other	1,832	1.9%	12,252,318	9,493,555	N/A
Grand Total	**98,181**	**100.0%**	**34,318,947**	**26,014,313**	
Total Hard shoreline	**77,621**	**78.4%**			
# pier pilings	63,768		11,867,854	9,324,493	0.01%

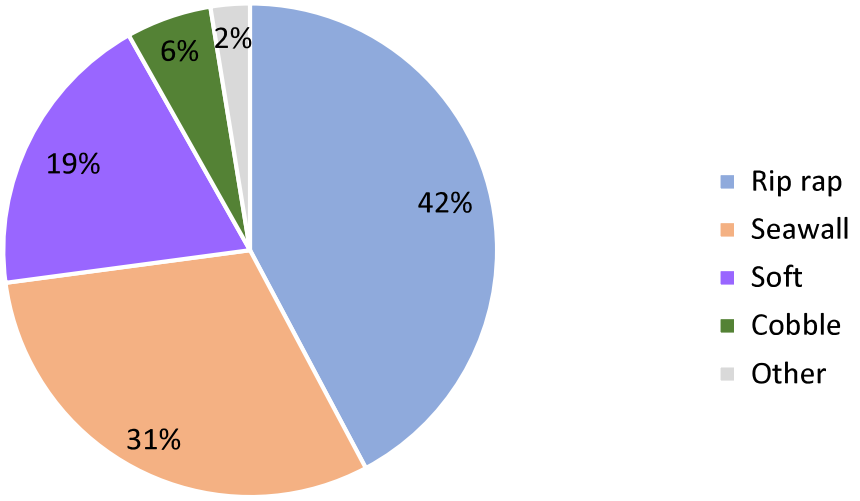

Figure 12. Percentage of shoreline habitat per habitat type along the perimeter of San Diego Bay, CA. "Other" includes pipes, chain-link fence, outfalls, boat launch ramps and unknown habitats that could not be determined from Google Earth satellite images. Importantly, pier pilings are not included in this perimeter figure but were quantified for bay-wide oyster abundance estimates.

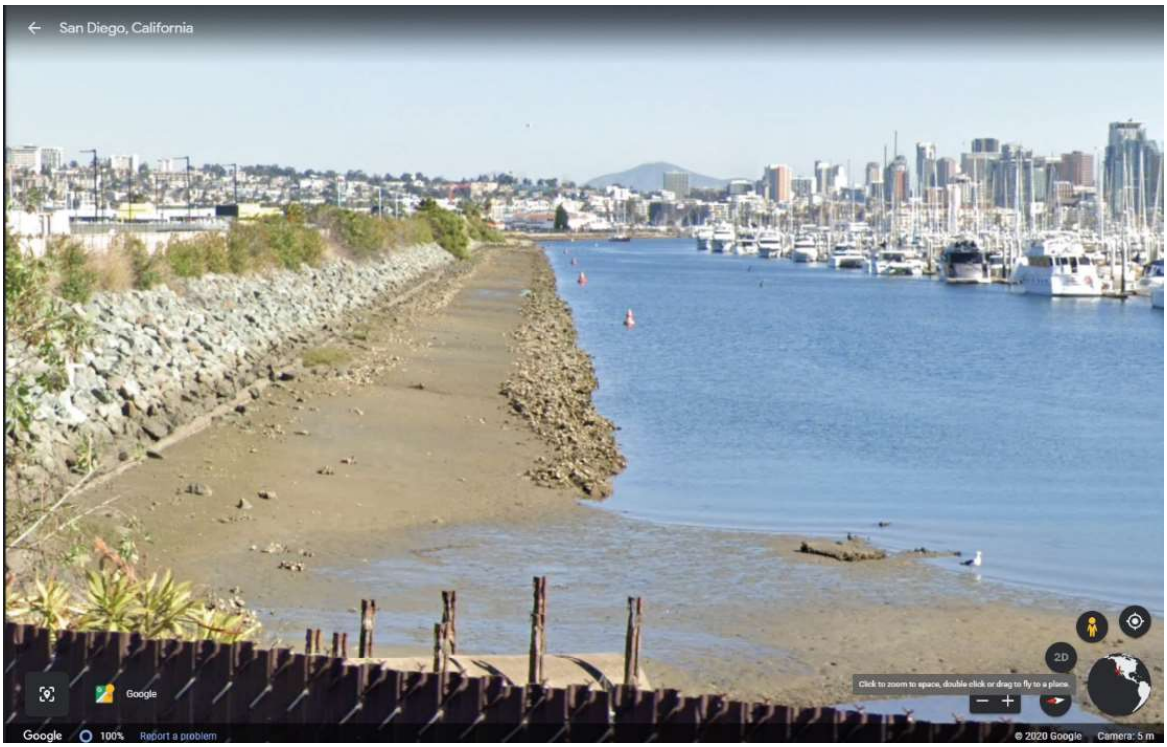

Figure 13. Possible oyster reef discovered below the rip rap in Harbor Island, San Diego Bay, CA.

Recruitment across sites and tidal elevations in 2020

In 2020, oyster recruitment was relatively low for both *O. lurida* and *C. gigas* compared to previous years. Importantly, no *Mytilus galloprovincialis* recruitment was observed.

O. lurida recruited exclusively to 0 m MLLW on the underside of horizontal concrete tiles across all sites in 2020, and at that elevation, their recruitment ranged from an average of 1.2 to 15 oysters on the undersides of tiles (2-way ANOVA, 2-way interaction, site*tide, p=0.0182, Figure 14). *O. lurida* recruited in highest abundances to tiles at ES compared to CV or LP at 0 m MLLW. *C. gigas* recruitment ranged from an average of 0 to 3 oysters per tile and recruited in highest abundance at ES but in equal abundances to 0 and 0.6 m MLLW (2-way ANOVA, site effect, p=0.0012, Figure 15). Importantly, at LP, the major space occupiers on the underside of horizontal concrete tiles were non-indigenous *Styela plicata* at 0 m MLLW and non-indigenous *Hydroides elegans* at 0.6 m MLLW (Figure 6, Appendix A).

A

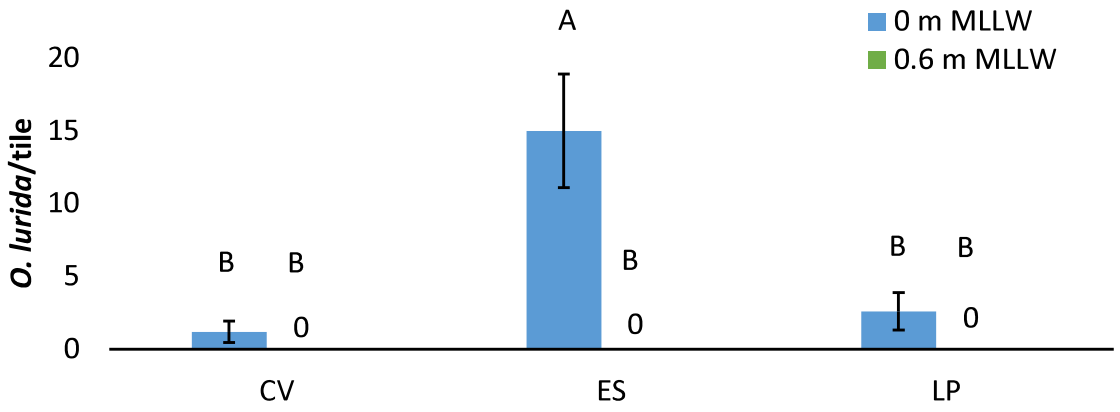

Figure 14. Number of *O. lurida* on the underside of horizontal concrete tiles deployed at 0 and +0.6 m MLLW in 2020 at sites in San Diego Bay, CA. Error bars=1 SE. Different letters above bars indicate statistically significant differences based upon post-hoc Tukey HSD tests.

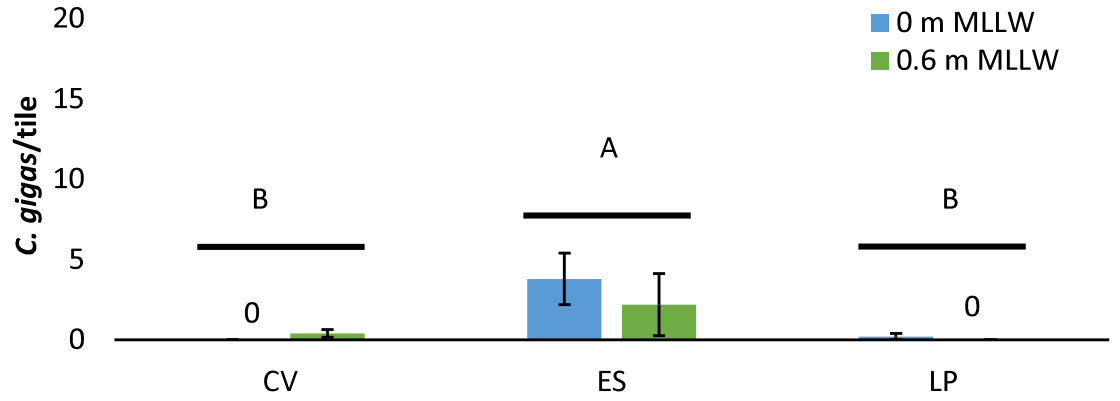

Figure 15. Number of *C. gigas* on the underside of horizontal concrete tiles deployed at 0 and +0.6 m MLLW in 2020 at sites in San Diego Bay, CA. Error bars=1 SE. Different letters above bars indicate statistically significant differences based upon post-hoc Tukey HSD tests.

Recruitment across years and tidal elevations at ES

To examine how the magnitude of 2020 oyster recruitment compared to previous years, we evaluated recruitment across a 6-year time period at ES on caged terra cotta tiles. *O. lurida* recruitment varied at ES across years and across tidal elevations, but sometimes the variation between elevations was more striking than in other years (2-way ANOVA, 2-way interaction, year*elevation, $p<0.0001$, Figure 16). *O. lurida* recruitment was the lowest in 2015 with an average of 2.4 *O. lurida*/tile, and the highest in 2018 with an average of 69.6 *O. lurida*/tile. No *O. lurida* were found at 0.6 m MLLW in any of the years. Similar to *O. lurida*, *C. gigas* had its lowest recruitment year in 2015 with an average of 0.12 oysters/tile and its highest recruitment in 2018 and 2019, where the highest average was 19.78 oysters/tile in 2019; it also consistently recruited in higher numbers to +0.6 m compared to 0 m MLLW (2-way ANOVA, effect of year, $p<0.0001$, and tidal elevation, $p<0.0001$, Figure 17). Qualitatively, *C. gigas* recruited in lower numbers than *O. lurida* across years

at ES, but recruited to both 0 and 0.6 m MLLW with highest abundances to 0.6 m MLLW (compare Y axes on Figures 16 and 17).

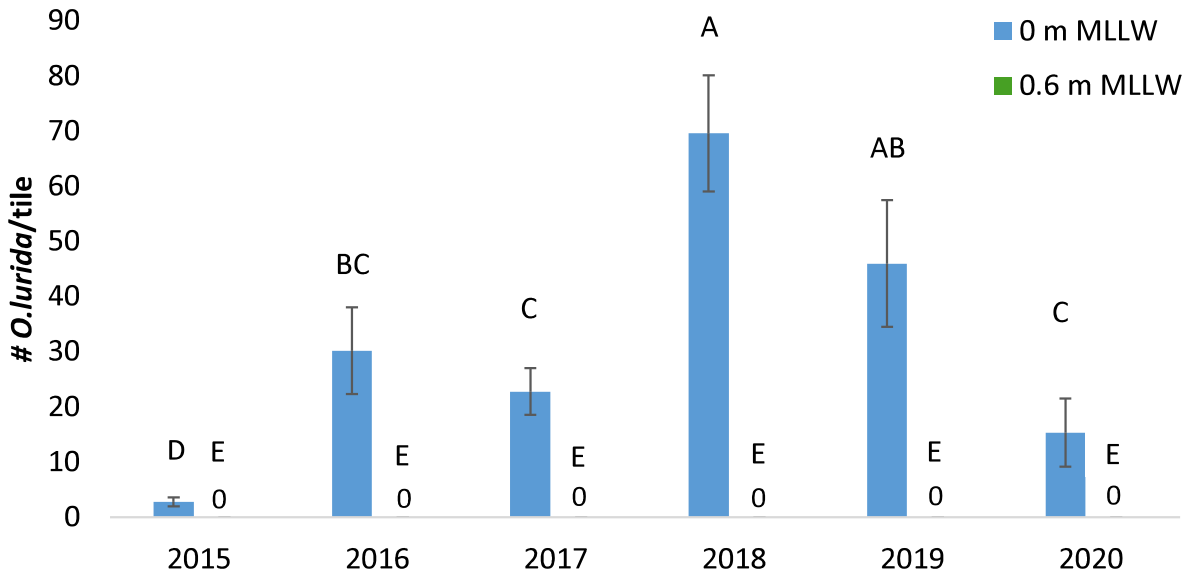

Figure 16. Number of *O. lurida* recruited to the bottom of caged terra cotta tiles deployed at 0 and +0.6 m MLLW during each recruitment season from 2015-2020 at E Street in San Diego Bay, CA. Error bars=1 SE. Different letters above bars indicate statistically significant differences based upon post-hoc Tukey HSD tests.

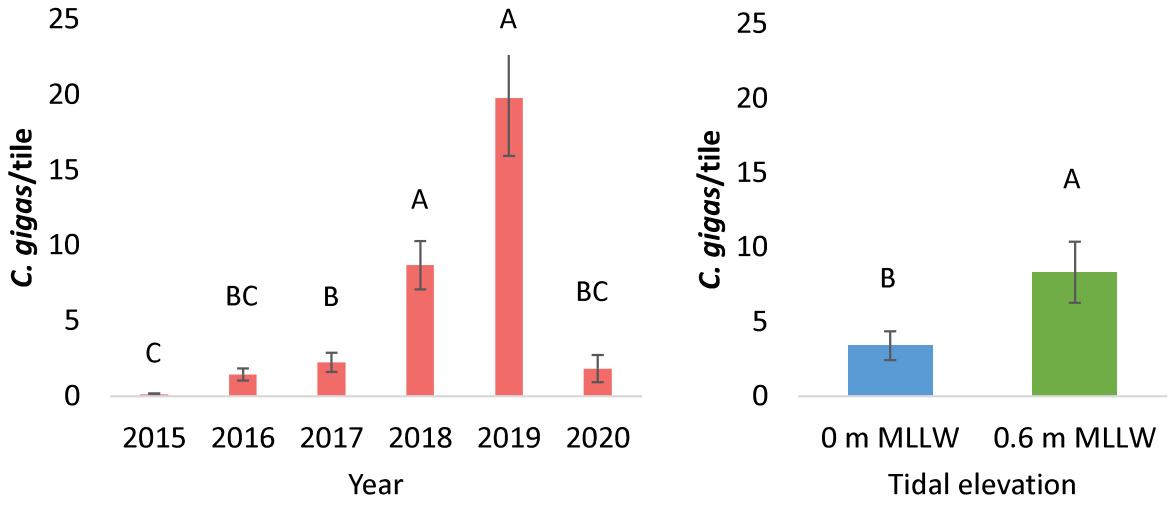

Figure 17. Number of *C. gigas* recruited to the bottom of caged terra cotta tiles deployed during each recruitment season from 2015-2020 (left) and at 0 and +0.6 m MLLW (right) at E Street in San Diego Bay, CA. Error bars=1 SE. Different letters above bars indicate statistically significant differences based upon post-hoc Tukey HSD tests.

Oyster recruitment across sites and years

To evaluate whether high recruitment years were consistent across sites, we examined archived recruitment data from caged terra cotta tiles at ES, GC and GB at 0 m MLLW from 2017-2019. High recruitment years for *O. lurida* were not consistent across sites at 0 m MLLW, and the magnitude for recruitment varied across sites, too. *O. lurida* recruitment was highest at ES in 2018 with 69.6 oysters/tile while highest recruitment at GC and GB was in 2017 with 145 oysters/tile and 16.8 oysters/tile, respectively (2-way ANOVA, 2-way interaction, site*year, $p<0.0001$, Figure 18). At GC and GB, *O. lurida* recruitment the lowest in 2019, but 2019 recruitment at ES was statistically equivalent to 2018, the highest recruitment year at ES. GC and GB show a negative trend of oyster recruitment across time, while ES does not follow that trend.

Like *O. lurida*, *C. gigas* recruitment strength was not consistent across years or sites. Recruitment was highest at ES in 2019 with an average of 11.6 oysters/tile but highest at GC in 2018, with 11.0 oysters/tile (2-way ANOVA, 2-way interaction, site*year, $p<0.0001$, Figure 19). At GB, no *C. gigas* recruited to tiles at 0 m MLLW during the evaluated time period. *C. gigas* recruitment was equally low across sites in 2017. Unlike *O. lurida*, *C. gigas* recruitment positively correlates with year for ES, but GC and GB do not follow a discernable trend.

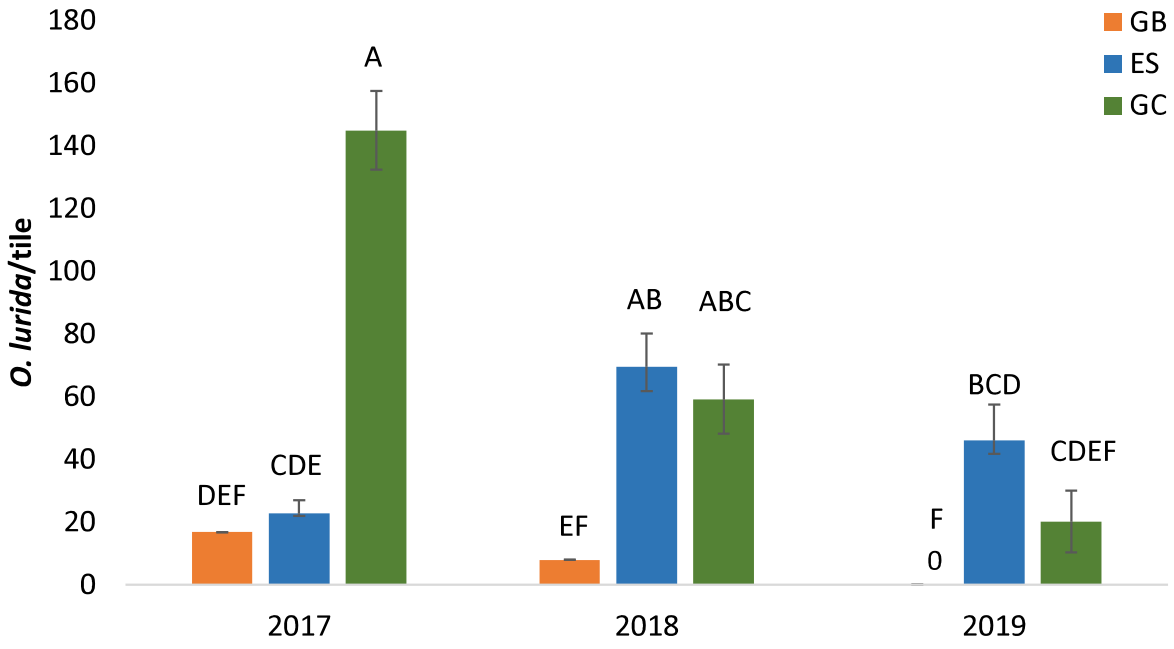

Figure 18. Number of *O. lurida* recruited to the undersides of terracotta tiles deployed at 0 m MLLW during the recruitment seasons of 2017-2019 in San Diego Bay sites, GB, ES, and GC. Error bars=1 SE. Different letters above bars indicate statistically significant differences based upon post-hoc Tukey HSD tests.

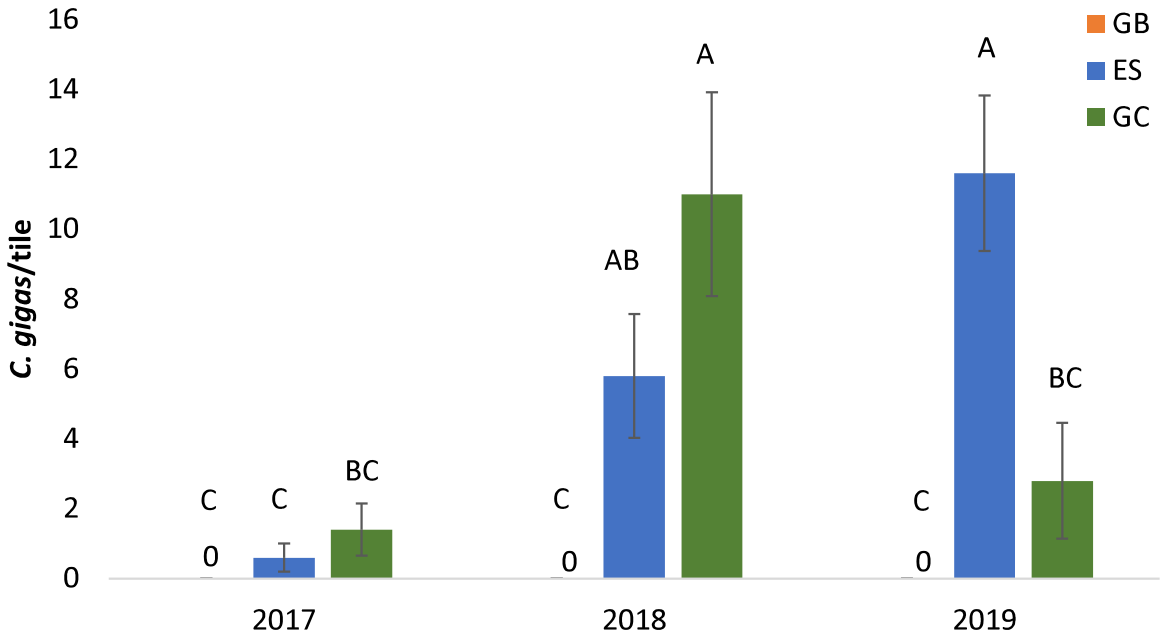

Figure 19. Number of *C. gigas* recruited to terracotta tiles deployed at 0 m MLLW during the recruitment seasons of 2017-2019 in San Diego Bay sites, GB, ES, and GC. Error bars=1 SE. Different letters above bars indicate statistically significant differences based upon post-hoc Tukey HSD tests.

Oyster recruitment across tile orientations and tidal elevations

In 2020, the magnitude of oyster recruitment was consistently low on all tile orientation treatments at 0 and 0.6 m MLLW across ES, LP, and CV, but generally trending to higher recruitment on the undersides of concrete tiles for both species.

At ES, average recruitment of *O. lurida*/tile was maximized at 15 oysters/tile and average *C. gigas* was maximized at 3.6 oysters/tile, both on the underside of horizontal tiles at 0 m MLLW. *O. lurida* recruited in abundances at least 9 times more to the underside of horizontal tiles compared to other treatments and tidal elevations (2-way ANOVA, 2-way interaction, treatment*tide, $p<0.0001$, Figure 20). *C. gigas* recruited in equal abundances across tidal elevations but recruited at least 5 times more to the underside of horizontal tiles relative to other treatments (2-way ANOVA, treatment effect, p=0. 0005; Figure 21).

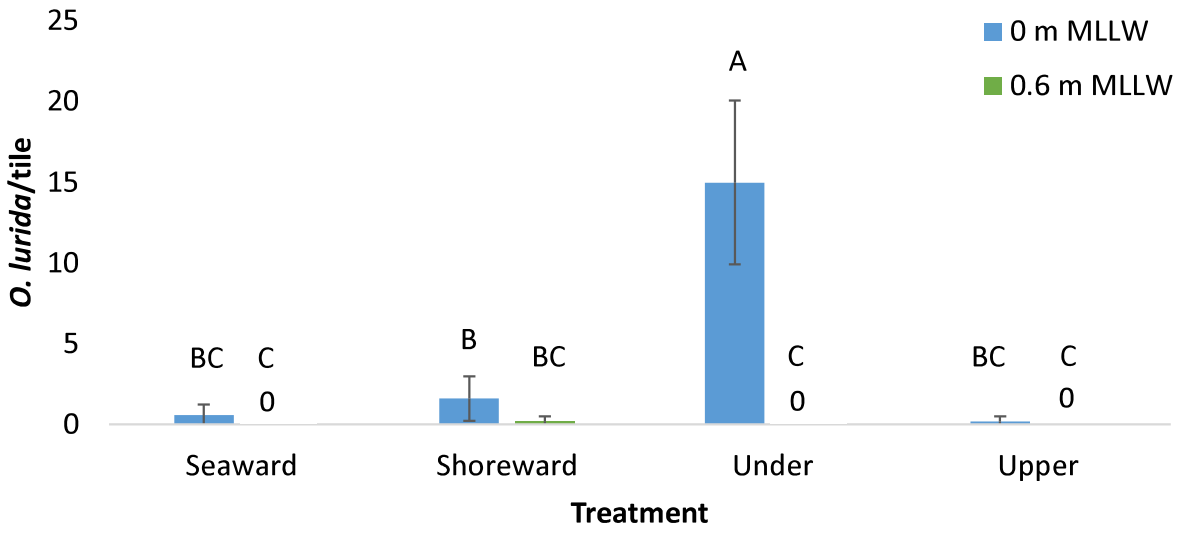

Figure 20. Number of *O. lurida* on concrete tile treatments deployed at various orientations at 0 and 0.6 m MLLW in 2020 at ES in San Diego Bay, CA. Shoreward and seaward-facing tiles were deployed vertically while under and upper refer to the underside and upper side of horizontally deployed tiles. Error bars=1 SE. Different letters above bars indicate statistically significant differences based upon post-hoc Tukey HSD tests.

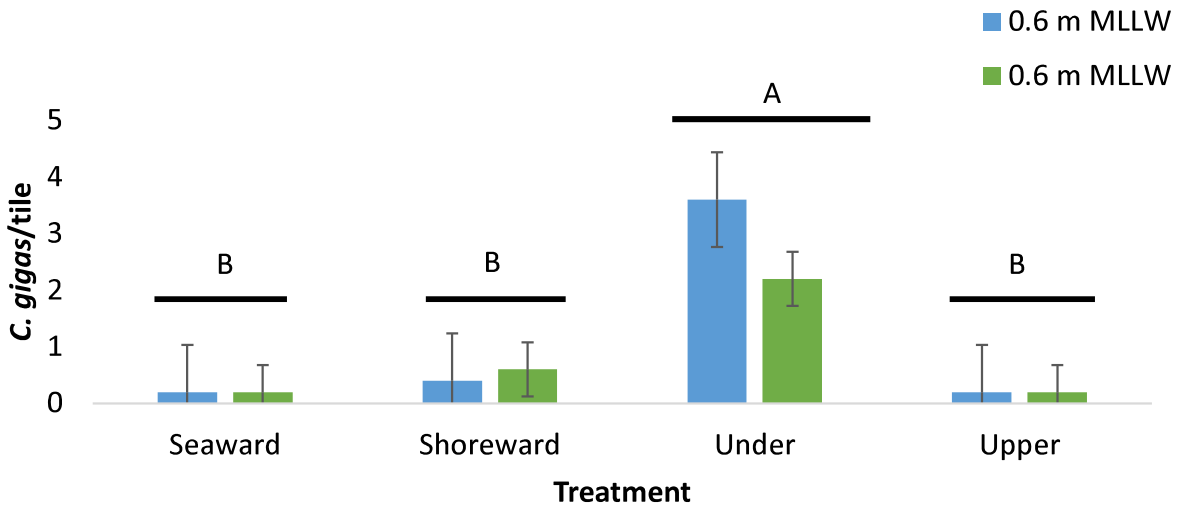

Figure 21. Number of *C. gigas* on concrete tile treatments deployed at various orientations at 0 and 0.6 m MLLW in 2020 at ES in San Diego Bay, CA. Shoreward and seaward-facing tiles were deployed vertically while under and upper refer to the underside and upper side of horizontally deployed tiles. Error bars=1 SE. Different letters above bars indicate statistically significant differences based upon post-hoc Tukey HSD tests.

At LP, *O. lurida* recruitment was maximized at 2.6 oysters/tile, again on the undersides, though the difference among treatments was not statistically significant; they did however, recruit statistically more at 0 m MLLW compared to 0.6 m MLLW (2-way ANOVA, effect of tidal elevation, p=0. 0011; Figure 22). *C. gigas* recruitment was low with a maximum average at 0.2 oysters/tile at LP, and there were no significant effects of tile orientation or tidal elevation on *C. gigas* recruitment (2-way ANOVA, all effects, p>0.05; Figure 23). *C. gigas* only recruited to the underside of tiles at 0 m MLLW and did not recruit to upper, seaward, and shoreward tile orientations at either tidal elevation at LP.

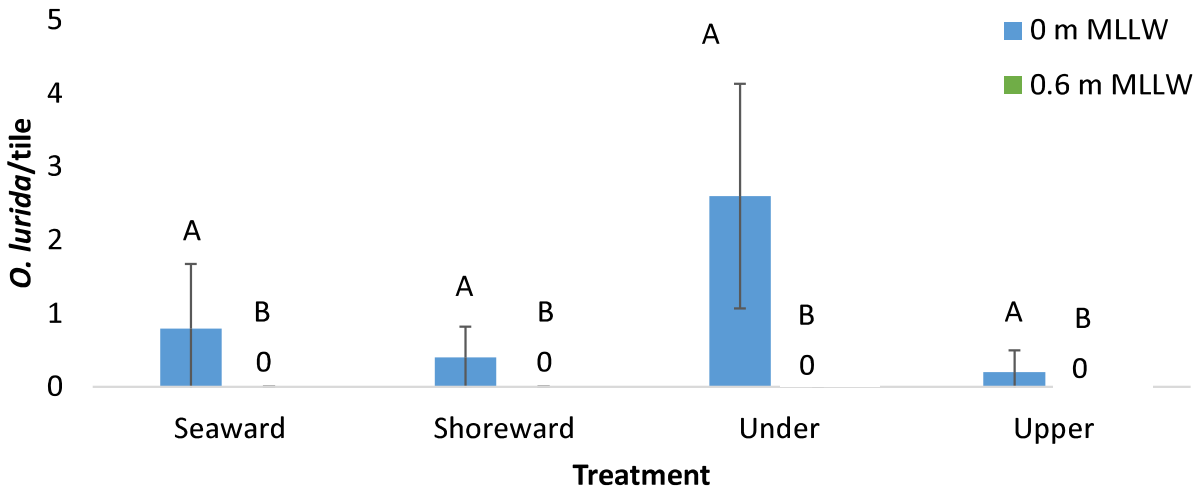

Figure 22. Number of *O. lurida* on concrete tile treatments deployed at various orientations at 0 and 0.6 m MLLW in 2020 at LP in San Diego Bay, CA. Shoreward and seaward-facing tiles were deployed

vertically while under and upper refer to the underside and upper side of horizontally deployed tiles. Error bars=1 SE. Different letters above bars indicate statistically significant differences based upon post-hoc Tukey HSD tests.

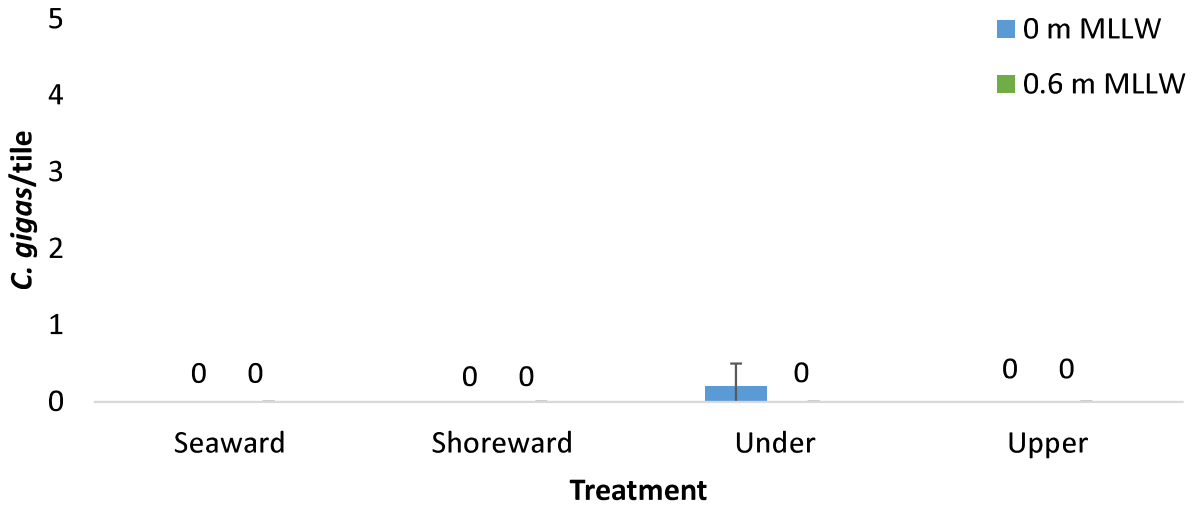

Figure 23. Number of *C. gigas* on concrete tile treatments deployed at various orientations at 0 and 0.6 m MLLW in 2020 at LP in San Diego Bay, CA. Shoreward and seaward-facing tiles were deployed vertically while under and upper refer to the underside and upper side of horizontally deployed tiles. Error bars=1 SE. Different letters above bars indicate statistically significant differences based upon post-hoc Tukey HSD tests.

At CV, *O. lurida* recruitment was maximized at 2.6 oysters/tile. Similar to LP, *O. lurida* at CV recruited in higher abundances to 0 m MLLW, but independent of tile orientation (2-way ANOVA, effect of tidal elevation, p=0. 0024; Figure 24). *C. gigas* recruitment was generally low and its average density ranged from 0 to 0.5 oysters/tile. Similar to LP, there was no significant effects of tile orientation or tidal elevation on *C. gigas* recruitment at CV (2-way ANOVA, all effects, p>0.05; Figure 25). *C. gigas* did not recruit to seaward or upper tiles at 0 or 0.6 m MLLW.

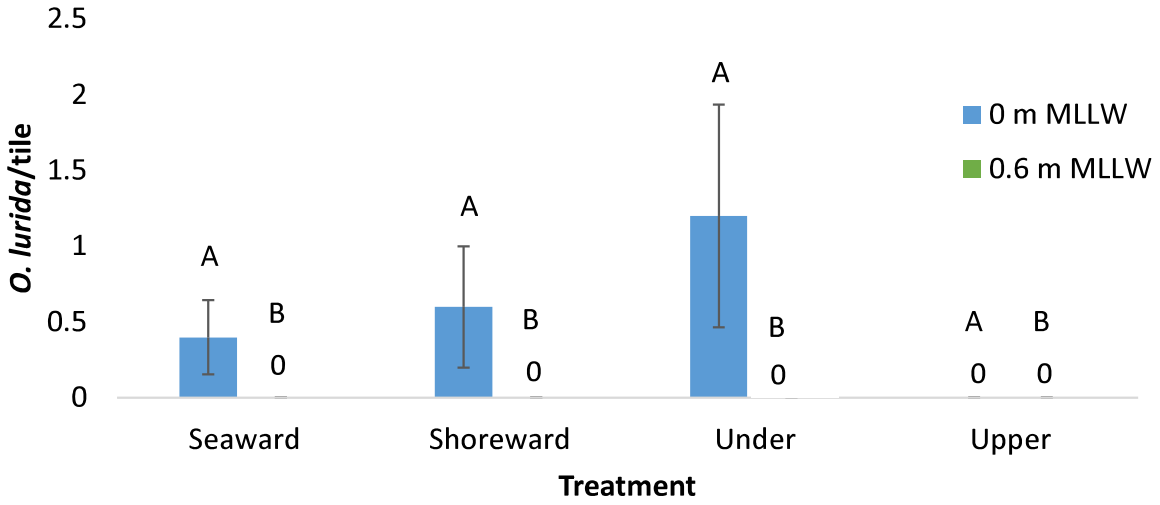

Figure 24. Number of *O. lurida* on concrete tile treatments deployed at various orientations at 0 and 0.6 m MLLW in 2020 at CV in San Diego Bay, CA. Shoreward and seaward-facing tiles were deployed vertically while under and upper refer to the underside and upper side of horizontally deployed tiles. Error bars=1 SE. Different letters above bars indicate statistically significant differences based upon post-hoc Tukey HSD tests.

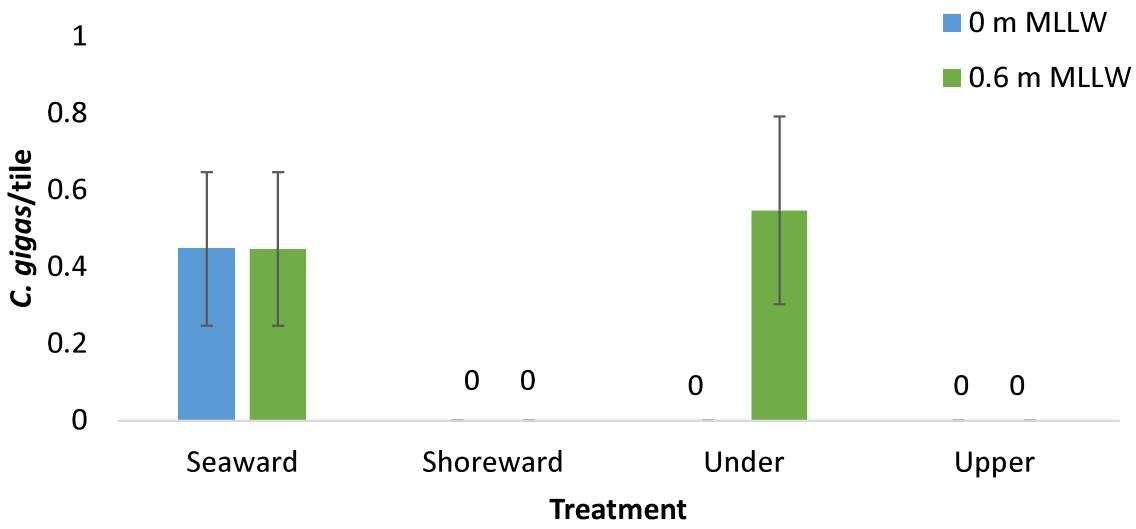

Figure 25. Number of *C. gigas* on concrete tile treatments deployed at various orientations at 0 and 0.6 m MLLW in 2020 at CV in San Diego Bay, CA. Shoreward and seaward-facing tiles were deployed vertically while under and upper refer to the underside and upper side of horizontally deployed tiles. Error bars=1 SE. Different letters above bars indicate statistically significant differences based upon post-hoc Tukey HSD tests.

DISCUSSION

We recorded the first-ever abundance estimate of oysters in San Diego Bay with a method that has not been attempted on oysters in southern California. Olympia oyster, *Ostrea lurida,* abundances have been estimated using the same method in Elkhorn Slough, CA (Kerstin Wasson, pers. comm.), but the oyster distribution, abundance, and habitat available in the intertidal are vastly different. There, *O. lurida* abundance has ranged from 1,000 to ~5,000 over the past decade likely because Elkhorn Slough experiences oyster recruitment failure during most years. *Crassostrea gigas* has not yet established in Elkhorn Slough. San Diego Bay, on the other hand, has experienced regular oyster recruitment success for the past 7 years, since we began regularly monitoring oyster recruitment, and has had an established *C. gigas* population since at least the early 2000s (Crooks et al. 2015). Our study establishes a critically important baseline (Knowlton & Jackson, 2008) for both oyster species in San Diego Bay, CA, that will be useful as environmental conditions within our local bays and estuaries shift in the face of global climate change (Scavia et al., 2002) and as habitat availability in the bay shifts due to human activity (Airoldi et al., 2005).

Despite being numerically abundant and common throughout southern California and especially within San Diego Bay (Tronske et al. 2018), neither *O. lurida* nor *C. gigas* exist in beds or reefs that would qualify as "oyster grounds" (sensu Zu Ermgassen et al. 2012), except in small patches at Kellogg Beach in the northern portion of San Diego Bay, and perhaps at Harbor Island (Figure 13), though the species composition of that habitat is currently unknown. Coast-wide, *O. lurida* oyster grounds and biomass are at less than 1% of their historical amounts, and this loss of habitat has resulted in the species being characterized as functionally extinct in a recent United States-wide survey (Zu Ermgassen et al. 2012).

Preliminary limited evidence across time suggests that *C. gigas* may be increasing in density and abundance within San Diego Bay, at least at some sites (Appendix B). Patterns of change for *O. lurida* were less pronounced, but *O. lurida* is known to vary dramatically in abundance from year to year, and has been known to experience large die-offs due to pronounced shifts in environmental factors, including salinity due to atmospheric rivers (Cheng et al., 2016). However, in a recent study in San Diego Bay, *O. lurida* was resilient to several atmospheric river events occurring in 2017 (unpublished, Appendix C). It will be critical to continue to monitor changes in density and abundance across time to better establish whether patterns we uncovered are robust or random.

Our data on shoreline armoring may indicate an increase in armored shorelines since 2013 – approximately 78.4% of San Diego Bay's shoreline is now armored with human-introduced habitat and this value is a slight increase from the 74% reported in 2013, though it is unclear whether the former estimate classified cobble as human-introduced, as we did here (U.S. Department of the Navy, Naval Facilities Engineering Command Southwest & Port of San Diego, 2013).

The analyses of the Google Earth perimeter revealed that pier pilings were profoundly under-sampled by our team, especially relative to the number of total piles (we sampled a mere 0.01% of the total) and relative to all other habitat types (Table 2), for which we were able to sample at least 0.5 % of total habitat. Future research efforts should emphasize an increase in sampling effort of pier piles across more sites so that we not only sample a greater percentage of the total number of piles but further, so that we get a more accurate estimate of bay-wide oyster densities on piles. Replacing pier pile oyster densities that we did record with seawall oyster densities had the effect of likely underestimating *O. lurida* abundance (since pier pile densities were 5 X higher than seawall densities) by more than 4.1 million oysters (12%) and overestimating *C. gigas* abundance (with pier pile densities 2 X lower than seawall densities) by about 6.6 million oysters (25%). Clearly, given the tremendously high number of pier piles as habitat in the bay, an accurate bay-wide oyster abundance estimate critically relies upon broader sampling of piles. To achieve comparable sampling effort to other habitats (sampling >0.5% of the habitat), we would need to sample a minimum of 320 piles.

For all of the habitats sampled for which we reported perimeter, we should ground-truth the observations (Kataoka et al., 2018). By ground-truthing the perimeter data, we can also better quantify lower tidal zones that are covered in water at the time of the Google Earth Imagery. Our perimeter data likely reflects the substrate available in higher intertidal zones, and represents a limitation to our current study that may overestimate habitat availability for *O. lurida* and artificially inflate our *O. lurida* abundance estimates.

We expanded oyster recruitment studies to LP and CV in 2020 and found that recruitment was exceedingly low, but an accumulation of our recruitment data across years shows that recruitment varies across years and sites, with poor relative recruitment in a particular year not being necessarily representative of all years. Oyster recruitment studies should continue at these sites to better understand the overall site-specific recruitment strength.

Moving forward, we can explore patterns from the data that were not analyzed in this report to better understand oyster distributions across habitat types, tidal elevations, and solar aspects in San Diego Bay (Table 3).

Table 3. Data analysis "bucket list" of analyses outside of the objectives of the report.

Priority	Analysis
1	Effect of area of the bay on adult oyster densities (North, North Central, South Central, South)
2	Effect of solar aspect on adult densities and recruitment
3	Percent cover of non-indigenous species versus native species on recruitment tiles and in surveys
5	Dead oyster vs. live oyster percent cover and recruitment as proxies for mortality
6	Size histograms of adult oysters and recruited oysters

ACKNOWLEDGEMENTS

We would like to acknowledge additional participants in the field and laboratory work including CSUF graduate students Valerie Goodwin and Brandon Quintana, plus a host of SCERP scholars and undergraduate student volunteers that aided in data recording while we were in the field. The San Diego Unified Port District and Merkel & Associates, Inc. provided funding and facilitated much-appreciated access to field sites.

REFERENCES

Airoldi, L., Abbiati, M., Beck, M. W., Hawkins, S. J., Jonsson, P. R., Martin, D., Moschella, P. S., Sundelöf, A., Thompson, R. C., & Åberg, P. (2005). An ecological perspective on the deployment and design of low-crested and other hard coastal defence structures. *Coastal Engineering*, *52*(10), 1073–1087.

Airoldi, L., Turon, X., Perkol-Finkel, S., & Rius, M. (2015). Corridors for aliens but not for natives: Effects of marine urban sprawl at a regional scale. *Diversity and Distributions*, *21*(7), 755–768.

Barrett, E. M. (1963). *The California oyster industry* (Vol. 123). Resources Agency of California, Department of Fish and Game.

Blum, J. C., Chang, A. L., Liljesthröm, M., Schenk, M. E., Steinberg, M. K., & Ruiz, G. M. (2007). The non-native solitary ascidian *Ciona intestinalis* (L.) depresses species richness. *Journal of Experimental Marine Biology and Ecology*, *342*(1), 5–14.

Bodkin, J. L., Coletti, H. A., Ballachey, B. E., Monson, D. H., Esler, D., & Dean, T. A. (2018). Variation in abundance of Pacific blue mussel (*Mytilus trossulus*) in the Northern Gulf of Alaska, 2006–2015. *Deep Sea Research Part II: Topical Studies in Oceanography*, *147*, 87–97.

Bonnot, P. (1935). The California oyster industry. *California Fish and Game*, *21*(1), 65–80.

Braby, C. E., & Somero, G. N. (2006). Ecological gradients and relative abundance of native (*Mytilus trossulus*) and invasive (*Mytilus galloprovincialis*) blue mussels in the California hybrid zone. *Marine Biology*, *148*(6), 1249–1262.

Buhle, E. R., & Ruesink, J. L. (2009). Impacts of invasive oyster drills on Olympia oyster (*Ostrea lurida* Carpenter 1864) recovery in Willapa Bay, Washington, United States. *Journal of Shellfish Research*, *28*(1), 87–96.

Bulleri, F., & Chapman, M. G. (2010). The introduction of coastal infrastructure as a driver of change in marine environments. *Journal of Applied Ecology*, *47*(1), 26–35.

Cheng, B. S., Chang, A. L., Deck, A., & Ferner, M. C. (2016). Atmospheric rivers and the mass mortality of wild oysters: Insight into an extreme future? *Proceedings of the Royal Society B: Biological Sciences*, *283*(1844), 20161462.

Coen, L. D., Brumbaugh, R. D., Bushek, D., Grizzle, R., Luckenbach, M. W., Posey, M. H., Powers, S. P., & Tolley, S. G. (2007). Ecosystem services related to oyster restoration. *Marine Ecology Progress Series*, *341*, 303–307.

Cornwell, W. K., & Ackerly, D. D. (2010). A link between plant traits and abundance: Evidence from coastal California woody plants. *Journal of Ecology*, *98*(4), 814–821.

Crooks, J. A., Crooks, K. R., & Crooks, A. J. (2015). Observations of the non-native Pacific oyster (*Crassostrea gigas*) in San Diego County, California. *California Fish and Game*, *101*(2), 101–107.

Dalrymple, D. J., & Carmichael, R. H. (2015). Effects of age class on N removal capacity of oysters and implications for bioremediation. *Marine Ecology Progress Series*, *528*, 205–220.

Defeo, O., & Rueda, M. (2002). Spatial structure, sampling design and abundance estimates in sandy beach macroinfauna: Some warnings and new perspectives. *Marine Biology*, *140*(6), 1215–1225.

Dodd Jr, C. K., & Dorazio, R. M. (200 . Using counts to simultaneously estima oundance and detection probabilities i a salamander community. *Herpetolo 60*(4), 468–478.

Fodrie, F. J., Rodriguez, A. B., Gittma , R. K., Grabowski, J. H., Lindquist, s. L., Peterson, C. H., Piehler, M. F., & Ridge, J. (2017). Oyster reefs as carbon ces and sinks. *Proceedings of the Royal Soc ty B: Biological Sciences*, *284* 9), 20170891.

Fofonoff, P. W., Ruiz, G. M., Steves, , Simkanin, C., & Carlton, (2018). *NEMESIS Database Species Summary*. National E otic Marine and Estuari pecies Information System. http://invasions.si.edu/nem is/

Gittman, R. K., Fodrie, F. J., Popowic A. M., Keller, D. runo, J. F., Currin, C. A., Peterson, C. H., & Piehler, M. F. (2015). E gineering awa natural defenses: An analysis of shoreline hardening in the U *Frontiers i logy and the Environment*, *13*(6), 301–307.

Goodsell, P. J., Chapman, M. G., & U derw , A. J. (2007). Differences between biota in anthropogenically fragment ha ts and in naturally patchy habitats. *Marine Ecology Progress Series*, *351* 3.

Moxley, J. H., Bogomolni, A., Hammill, M. O., Moore, K. M. T., Polito, M. J., Sette, L., Sharp, W. B., Waring, G. T., Gilbert, J. R., Halpin, P. N., & Johnston, D. W. (2017). Google haul out: Earth observation imagery and digital aerial surveys in coastal wildlife management and abundance estimation. *BioScience*, *67*(8), 760–768.

NOAA Fisheries. (2020, December 18). *Understanding Living Shorelines | NOAA Fisheries* (National). NOAA. https://www.fisheries.noaa.gov/insight/understanding-living-shorelines

Padilla, D. K. (2010). Context-dependent impacts of a non-native ecosystem engineer, the Pacific oyster *Crassostrea gigas*. *Integrative and Comparative Biology*, *50*(2), 213–225.

Peterson, B. J., & Heck Jr, K. L. (1999). The potential for suspension feeding bivalves to increase seagrass productivity. *Journal of Experimental Marine Biology and Ecology*, *240*(1), 37–52.

Polson, M. P., & Zacherl, D. C. (2009). Geographic distribution and intertidal population status for the Olympia oyster, *Ostrea lurida* Carpenter 1864, from Alaska to Baja. *Journal of Shellfish Research*, *28*(1), 69–77.

Pooler, P. S., & Smith, D. R. (2005). Optimal sampling design for estimating spatial distribution and abundance of a freshwater mussel population. *Journal of the North American Benthological Society*, *24*(3), 525–537.

Pyšek, P., Hulme, P. E., Simberloff, D., Bacher, S., Blackburn, T. M., Carlton, J. T., Dawson, W., Essl, F., Foxcroft, L. C., Genovesi, P., Jeschke, J. M., Kühn, I., Liebhold, A. M., Mandrak, N. E., Meyerson, L. A., Pauchard, A., Pergl, J., Roy, H. E., Seebens, H., … Richardson, D. M. (2020). Scientists' warning on invasive alien species. *Biological Reviews*, *95*(6), 1511–1534.

Ruiz, G. M., Carlton, J. T., Grosholz, E. D., & Hines, A. H. (1997). Global invasions of marine and estuarine habitats by non-indigenous species: Mechanisms, extent, and consequences. *American Zoologist*, *37*(6), 621–632.

Scavia, D., Field, J. C., Boesch, D. F., Buddemeier, R. W., Burkett, V., Cayan, D. R., Fogarty, M., Harwell, M. A., Howarth, R. W., Mason, C., Reed, D. J., Royer, T. C., Sallenger, A. H., & Titus, J. G. (2002). Climate change impacts on U.S. coastal and marine ecosystems. *Estuaries*, *25*(2), 149–164.

Scanes, E., Johnston, E., Cole, V., O'Connor, W., Parker, L., & Ross, P. (2016). Quantifying abundance and distribution of native and invasive oysters in an urbanised estuary. *Aquatic Invasions*, *11*(4), 425–436.

Shaw, W. N. (1997). The shellfish industry of California—Past, present and future. *NOAA Tech. Rep. NMFS*, *128*, 57–74.

Shinen, J. S., & Morgan, S. G. (2009). Mechanisms of invasion resistance: Competition among intertidal mussels promotes establishment of invasive species and displacement of native species. *Marine Ecology Progress Series*, *383*, 187–197.

Trimble, A. C., Ruesink, J. L., & Dumbauld, B. R. (2009). Factors preventing the recovery of a historically overexploited shellfish species, *Ostrea lurida* Carpenter 1864. *Journal of Shellfish Research*, *28*(1), 97–106.

Tronske, N. B., Parker, T. A., Henderson, H. D., Burnaford, J. L., & Zacherl, D. C. (2018). Densities and zonation patterns of native and non-indigenous oysters in southern California Bays. *Wetlands*, *38*(6), 1313–1326.

Tyrrell, M. C., & Byers, J. E. (2007). Do artificial substrates favor nonindigenous fouling species over native species? *Journal of Experimental Marine Biology and Ecology*, *342*(1), 54–60.

U.S. Department of the Navy, Naval Facilities Engineering Command Southwest & Port of San Diego. (2013). *San Diego Bay Integrated Natural Resources Management Plan, Final September 2013*.

Williams, R. O. B., Hedley, S. L., Branch, T. A., Bravington, M. V., Zerbini, A. N., & Findlay, K. P. (2011). Chilean blue whales as a case study to illustrate methods to estimate abundance and evaluate conservation status of rare species. *Conservation Biology*, *25*(3), 526–535.

Van Dyke, E., & Wasson, K. (2005). Historical ecology of a central California estuary: 150 years of habitat change. *Estuaries*, *28*(2), 173–189.

Wells, S. R., Wing, L. C., Smith, A. M., & Smith, I. W. G. (2019). Historical changes in bivalve growth rates indicate ecological consequences of human occupation in estuaries. *Aquatic Conservation: Marine and Freshwater Ecosystems*, *29*(9), 1452–1465.

Zohar, Y., Hines, A. H., Zmora, O., Johnson, E. G., Lipcius, R. N., Seitz, R. D., Eggleston, D. B., Place, A. R., Schott, E. J., Stubblefield, J. D., & Chung, J. S. (2008). The Chesapeake Bay Blue crab (*Callinectes sapidus*): A Multidisciplinary Approach to Responsible Stock Replenishment. *Reviews in Fisheries Science*, *16*(1–3), 24–34.

Zu Ermgassen, Philine S. E., Spalding, M. D., Blake, B., Coen, L. D., Dumbauld, B., Geiger, S., Grabowski, J. H., Grizzle, R., Luckenbach, M., McGraw, K., Rodney, W., Ruesink, J. L., Powers, S. P., & Brumbaugh, R. (2012). Historical ecology with real numbers: Past and present extent and biomass of an imperilled estuarine habitat. *Proceedings of the Royal Society B: Biological Sciences*, *279*(1742), 3393–3400.

Zu Ermgassen, P.S.E., Hancock, B., DeAngelis, B., Greene, J., Schuster, E., Spalding, M., & Brumbaugh, R. (2016). Setting objectives for oyster habitat restoration using ecosystem services: A manager's guide. *The Nature Conservancy: Arlington, VA, USA*.

Appendix A

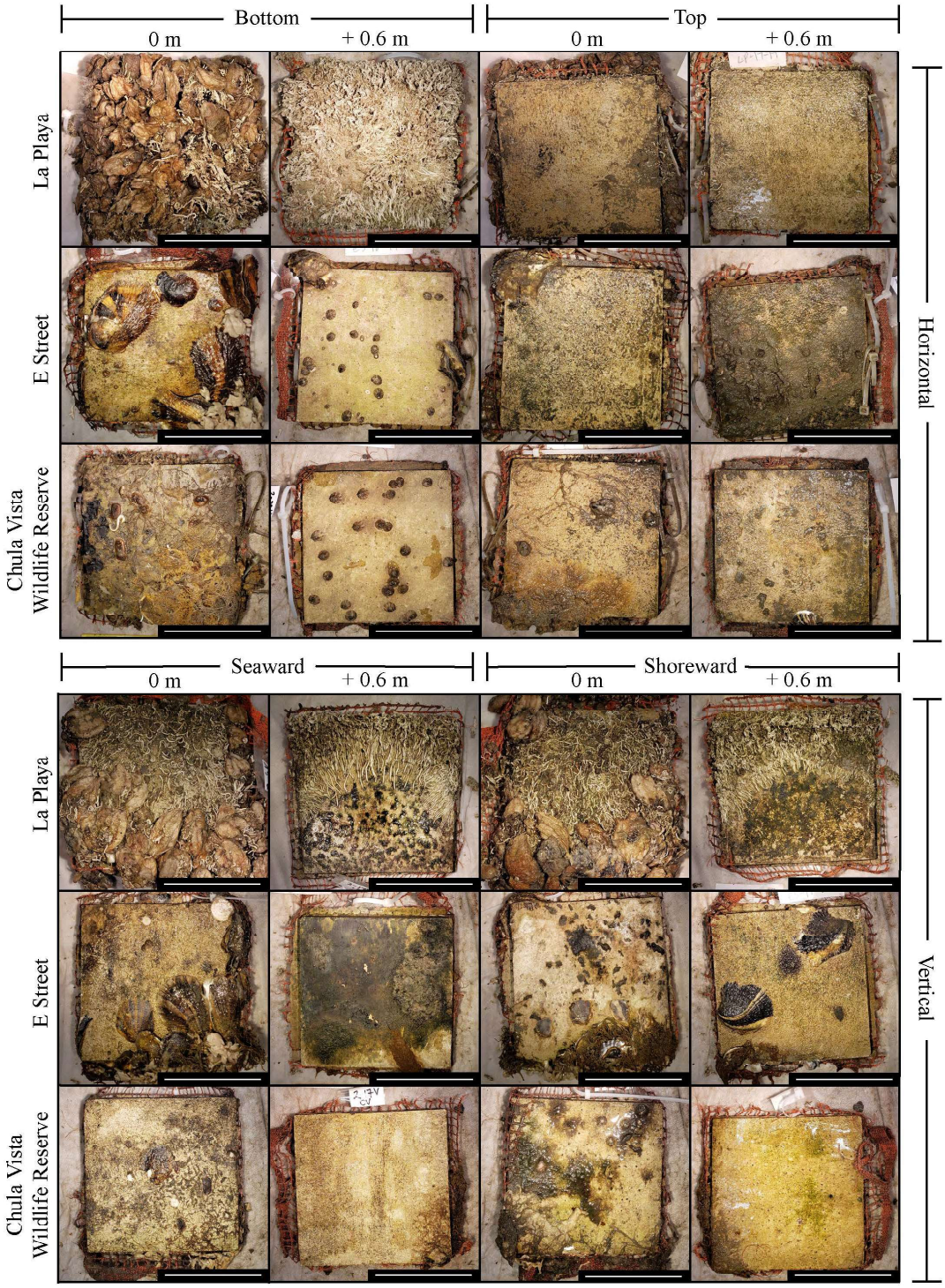

Figure A. Treatment tiles post-deployment on the horizontally orientated tiles underside, upper side, and vertically orientated tiles facing seaward and shoreward at low (0 m) and high (0.6 m) tidal elevations. Tiles were deployed at La Playa (LP), E Street (ES), and Chula Vista Wildlife Reserve (CV) in San Diego Bay, CA from March to October 2020. Scale bar = 10 cm.

Appendix B – Research Poster – Smith et al. 2020

Appendix C – Research Poster – Suther et al. 2017

Density and abundance of native and non-native oysters *Ostrea lurida* and *Crassostrea gigas* over time in San Diego Bay, California

Jada E. Smith, Joann G. Lam, Madison E. Panzino, Trina R. Miller, Alisa R. Hernandez, Nicholas J. Torres, Dr. William J. Hoese, Dr. Danielle C. Zacherl

CALIFORNIA STATE UNIVERSITY FULLERTON

CSU Fullerton Southern California Ecosystems Research Program

Introduction

- Oysters are a foundation species in intertidal estuaries[1]
  - Create complex habitat and stabilize shorelines[2]
- Oyster bed habitat has declined 85% at a global scale[1]
- The U.S. west coast's only native oyster species, *Ostrea lurida*[3], declined to function extinction by early 1900s (Fig. 1)[4]
- In recent decades, global invader *Crassostrea gigas* established in southern California[5,6] and has recently and radically increased abundance and density in Newport Bay, CA (D. Zacherl 2020, unpub. data) (Fig. 2)

Figure 1. *O. lurida.*

Figure 2. *C. gigas.*

Research Question

- Have densities and abundances of *C. gigas* and *O. lurida* increased since 2013?
  - Hypothesis: Since 2013, *C. gigas* densities and abundances have increased, while *O. lurida* densities and abundances have decreased

Methods

- Data collected in San Diego Bay, CA in 2013/14, 2017, 2020: Chula Vista Wildlife Reserve (CV), Grand Caribe (GC), Glorietta Bay (GB) (Fig. 3)
- To estimate oyster density, quadrats at CV and GC (0.25 m^2) and at GB (0.075 m^2) randomly placed along 18-50 m transects at randomly selected tidal elevations ranging from -0.31 to 1.81 m MLLW
- Tidal elevations estimated per quadrat using LaserMark LM-30 laser
- Abundance of *O. lurida* and *C. gigas* at each site per year calculated by multiplying total area of habitat available by oyster species density
- Differences across years on *O. lurida* and *C. gigas* density each tested using one-way analysis of variance (ANOVA) in JMP 14.0 separately for lower (≤ +0.38 m MLLW) and higher tidal elevations (> +0.38 m MLLW)
- Data in 2020 collected using COVID-19 safe protocols; data collectors communicated with data recorders via Zoom video call (Fig. 4)

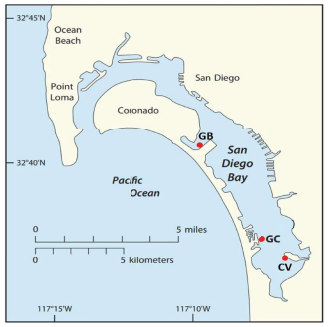

Figure 3. Map of study sites in San Diego Bay, California.

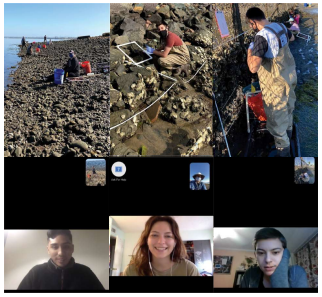

Figure 4 COVID-19 safe data collection at CV, GC, and GB (left to right). N. Torres, M. Panzino, and T. Miller recording data via Zoom video (left to right).

Results

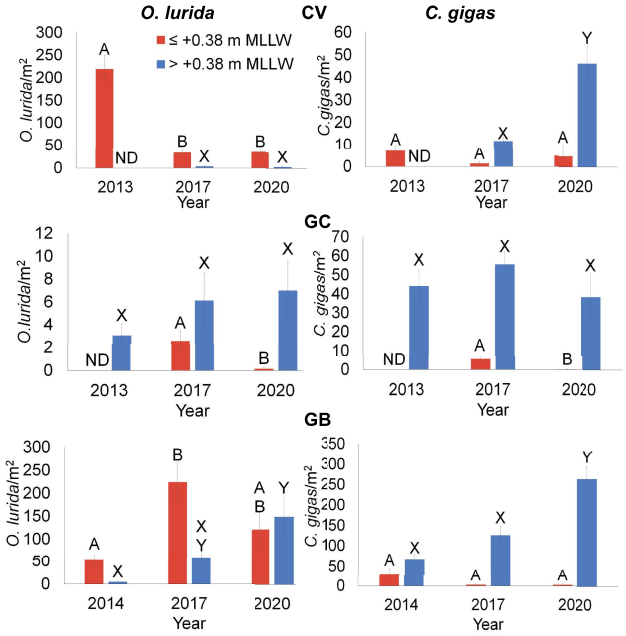

Figure 5. Densities of *Ostrea lurida* (left) and *Crassostrea gigas* (right) at lower (red bars) and higher (blue bars) tidal elevations for 2013-2020 at Chula Vista Wildlife Reserve (CV, upper panel) and Grand Caribe (GC, middle panel) and 2014-2020 at Glorietta Bay (GB, lower panel). Error bars equal ±1SE. Bars not connected by the same letter are significantly different from each other. ND equals no data.

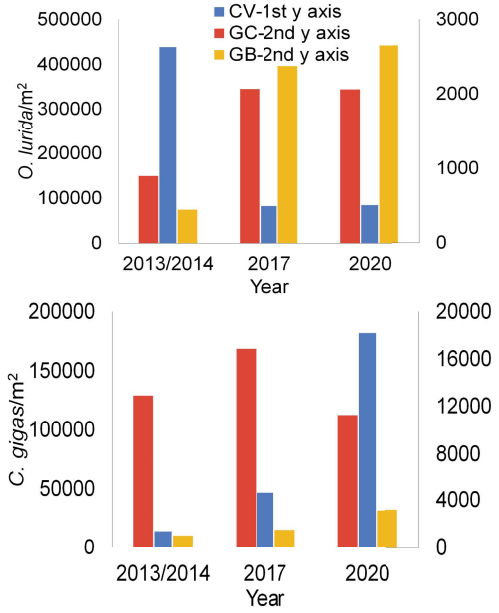

Figure 6. *Ostrea lurida* and *Crassostrea gigas* abundances at Chula Vista Wildlife Reserve (CV), Grand Caribe (GC), and Glorietta Bay (GB) for the years 2013/2014, 2017, and 2020. CV abundance is plotted on the primary axis while GC and GB abundances are plotted on the secondary axis. Note the much higher abundances at CV is due to significantly more habitat.

- *O. lurida* densities and abundances within each site fluctuated from year to year with no overall trend apparent; total abundance across all sites declined 3.7 times (Figs. 5, 6)
- *C. gigas* densities and abundances increased at two of three sites (CV, GB) and remained the same at one site (GC); total abundance across all sites increased 5.5 times (Figs. 5, 6)

Discussion

- Populations of *C. gigas* are thriving and overall abundances have significantly increased as in Newport Bay, CA (Fig. 7). We predict the lack of increase in population density at the third site may be due to lack of available substrata.
- Because *C. gigas* is a known global invader with sometimes negative impacts on native fauna, our data provides an important benchmark for future studies on its establishment trajectory in southern California estuaries.
- There is not a clear relationship between changes in *C. gigas* and *O. lurida* densities across all sites. This may be due to the fact that their distributions do not completely overlap[6]
- One study showed a negative impact on *O. lurida* when the two species compete in overlapping tidal zones[7]. Further studies could validate these findings.

Figure 7. *C. gigas* dominated the upper intertidal landscape.

Acknowledgments

We would like to thank Dr. Zacherl's lab: Marah Wolfe, Ty Frantz, Chelsea Bowers, and Bryce Perog for helping us collect data on-site for each location and Julia Teeple and Mayra Silva from the SCERP 2019 cohort for helping us record data. We would also like to thank the benefactors of the SCERP program for their help in supporting this research; BEIM foundation, Dr. Michael Horn and other philanthropic donations, CSUF college of Natural Sciences and Mathematics and Department of Biological Science Drs. Johnson, Walker, Casem, Burnaford. Funding was provided to DZ via Merkel and Associates, Inc. via flow through from Port of San Diego.

Literature Cited

1. Beck, M. W., Brumbaugh, R. D., Airoldi, L., Carranza, A., Coen, L. D., Crawford, C., . . . Guo, X. (2011). *BioScience, 61*(2), 107-116. doi:10.1525/bio.2011.61.2.5
1. Ramsay, J. (2012). [Unpublished master's thesis]. Oregon State University.
2. Pritchard, C., Shanks, A., Rimler, R., Oates, M., and Rumrill, S. (2015). *Journal of Shellfish Research* 34(2), 259-271. https://doi.org/10.2983/035.034.0207
3. White, J., Ruesink, J. L., & Trimble, A. C. (2009). *Journal of Shellfish Research, 28*(1), 43-49. doi:10.2983/035.028.0109
4. Crooks, J. A., Crooks, K. R., & Crooks, A. J. (2015). *California Fish and Game, 101*(2), 101-107.
5. Tronske, N. B., Parker, T. A., Henderson, H. D., Burnaford, J. L., & Zacherl, D. C. (2018). *Wetlands, 38*(6), 1313-1326. doi:10.1007/s13157-018-1055-0
6. Buhle, E. R., & Ruesink, J. L. (2009). *Journal of Shellfish Research, 28*(1), 87-96. doi:10.2983/035.028.0115

The Impact of Atmospheric River Events on *Ostrea lurida* and *Crassostrea gigas* Densities in Southern California Estuaries

Holly Suther, Jacob Javier, Shannon Chou, Brittany Cook, Daniel Jaques, William J. Hoese, and Danielle C. Zacherl
Department of Biological Sciences, California State University, Fullerton

Introduction

- Oyster reefs have globally declined an estimated 85% from historic levels, provoking restoration efforts in Southern California's estuaries.[1]
- Oyster reefs composed of native *Ostrea lurida* and non-native *Crassostrea gigas* (Fig. 1) could increase habitat diversity[2][3] and provide shoreline stabilization[4] to local estuaries.
- Estuaries are a mixture of freshwater and saltwater, a proportion that is influenced by large inputs of freshwater from sources like large precipitation events.
- In 2011, *O. lurida* population densities declined in San Francisco Bay after salinity dropped below the tolerance threshold (6.3ppt for 8days) from a large input of freshwater that followed an atmospheric river (AR) event.[5]
  - ARs are long narrow corridors of water vapor (<1000km x >2000km x >20mm)

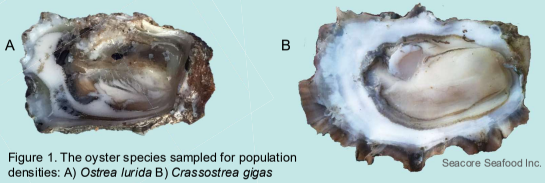

Figure 1. The oyster species sampled for population densities: A) *Ostrea lurida* B) *Crassostrea gigas*

Hypotheses

- Environmental factors (e.g. salinity, pH, etc.) influenced by AR-related precipitation events are linked to declines in Southern California oyster population densities.
- Native *Ostrea lurida* will show a greater decline in population density than non-native *Crassostrea gigas* due to environmental factors influenced by AR events.

Methods

Biological Measurements

- Oyster population density data were collected at four sites in Newport Bay and San Diego Bay in Dec 2016-Jan 2017 and again in May 2017. (Fig. 2)
- Population densities were counted with 0.25m^2 quadrats (n=30) placed randomly along 50m and 30m transects. (Fig. 2)
  - Alternate quadrats sized 0.045m^2 were utilized at 15th Street due to a vertical wall that intersected the transect lines.
- Transect lines ran across varying tidal elevations (-0.3m, 0.0m, +0.3m, +0.6m) from MLLW.
  - Tidal elevations chosen based on previously-observed dense populations of both species.
- For use in future studies, substrate data were recorded using a 49 point intersected quadrat at each site for each quadrat location. (Fig. 2)

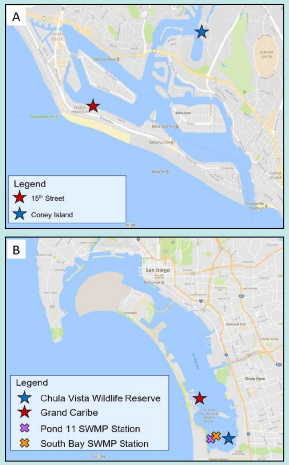

Figure 2. Locations surveyed in A) Newport Bay (NP) consisted of 15th Street and Coney Island. B) San Diego Bay (SD) locations were Chula Vista Wildlife Reserve and Grand Caribe. C) Substrate surveyed using a 49 point-contact quadrat off 0m MLLW transect.

Methods cont.

Physical Measurements

- AR events were identified by satellite imaging courtesy of the Center for Western Weather and Water Extremes. (Fig. 3)
- Daily precipitation and air temperature data were collected by NOAA's National Centers for Environmental Information for San Diego and Newport.
- Water quality data (salinity, pH, dissolved oxygen, water temperature) were measured in 15 minute intervals by the National Estuarine Research Reserves Systems (NERRS).

Statistics

- A three-way ANOVA test was performed via JMP 13.1.0 software for both sites in SD for tidal elevation (GC=+0.3m,+0.6m; CV=0.0m,+0.3m), species (*O. lurida* and *C. gigas*), and date (January and May)
- All oyster population density data was fourth root transformed to minimize the heteroscedasticity of the data.
- Multiple t-tests (two samples, one tailed, unequal variance) were performed for the 0.0m MLLW tidal elevation in NP to analyze oyster population densities for both species and at both sites.

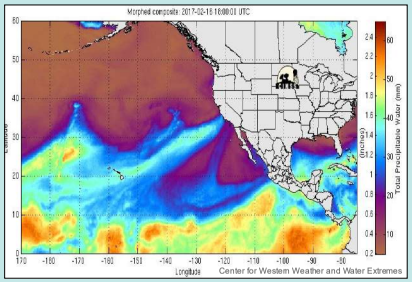

Figure 3. Atmospheric river events impacting the west coast on February 16, 2017. Southern California was forecasted to receive 1-4.5 inches of precipitation over the 72 hours following the AR event. Both Newport Bay and San Diego Bay were impacted by these AR events.

Results

- Several AR events occurred from December 2016 to March 2017, leading to precipitation that fell within the San Diego Bay or Newport Bay watersheds. (Fig. 4)
- Following each AR event was a surge in rainfall, which co-occurred with potentially lethal drops in salinity and pH but for non-lethal durations. (Fig. 4).
- *Crassostrea gigas* declined significantly at the +0.3m MLLW tidal elevation, for all sites except 15th Street. (Fig. 5; CV: P<0.0005, GC: P<0.1983, Coney: P<0.02436, 15th: P<0.1098)
- *Ostrea lurida* population density did not change significantly at any tidal elevation at any of the four sites. (Fig. 5, 3-way ANOVA post-hoc Tukey comparisons and t-tests, p<0.05)

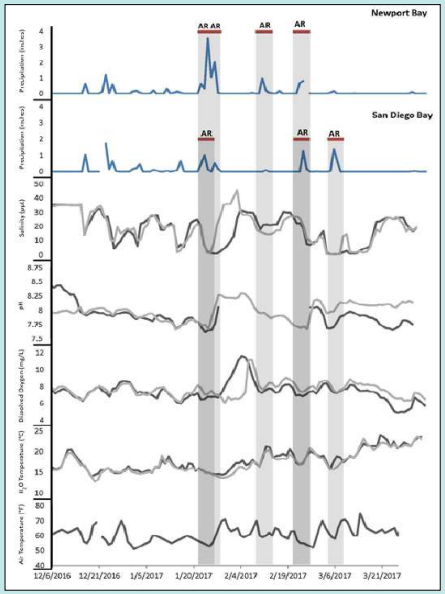

Figure 4. Precipitation (inches) data with indicated AR events for Newport Bay and San Diego Bays (top two panels) with water quality parameters for San Diego Bay over the same time period: minimum salinity (ppt), pH, dissolved oxygen (mg/L), water temperature (degrees Celsius), and air temperature (degrees Fahrenheit). All figures range from December to March 2017. Water quality data are sourced from both Pond 11 (dark gray) and South Bay (light gray) weather stations in San Diego Bay, CA. Precipitation and AR data for Newport Bay.

Results cont.

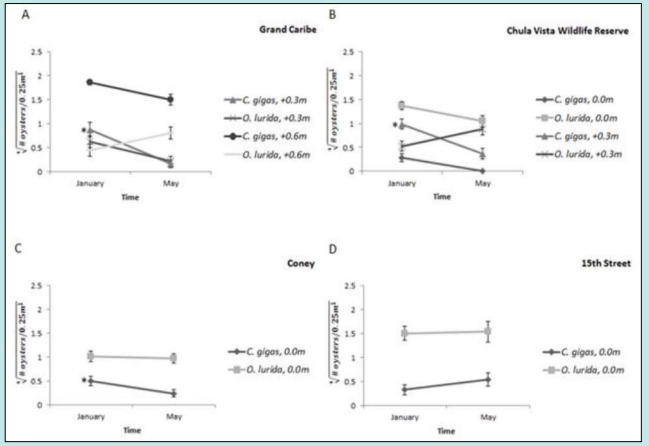

Figure 5. Graph representing change in population density of *Ostrea lurida* and *Crassostrea gigas* from January to May, 2017. Oyster population density to the fourth root per 0.25m^2 shown as a function of time. A) Grand Caribe, San Diego Bay at +0.3m and +0.6m tidal elevations B) Chula Vista Wildlife Reserve, San Diego Bay at 0.0m and +0.3m tidal elevations C) Coney Island, Newport Bay at 0 m tidal elevation D) 15th Street, Newport Bay at 0.0m tidal elevation. Asterisks indicate significant change in oyster population density for the given species at specific tidal elevation.

Conclusion

- Although water quality did drop to lethal levels on multiple occasions, no drop was for the necessary duration to be considered lethal.
- Native *Ostrea lurida* may be more acclimatized to local AR events than recently introduced *Crassostrea gigas*, or *C. gigas* declines may be due to another unknown factor.
- Water quality data was incomplete for all sites and will need further collection in order to form a clearer relationship between water quality and AR events.
- San Francisco Bay may be more susceptible to AR impacts on oysters by experiencing more extreme ARs and having a larger watershed; both can lead to more significant impacts on estuarine water quality.
- By finding relationships between AR events and oyster mortalities, restoration efforts can be directed towards areas better suited for oyster reefs.

Literature Cited

1. Beck, M., Brumbaugh, R., Airoldi, L., Carranza, A., Coen, L., Crawford, C., Defeo, O., *et al.* (2011). Oyster Reefs at Risk and Recommendations for Conservation, Restoration, and Management. BioScience, 63(12), 107–116.
2. Beck, M. W., Heck K.L., J., Able, K. W., Childers, D. L., Eggleston, D. B., Gillanders, B. M., ... Weinstein, M. P. (2001). The identification, conservation, and management of estuarine and marine nurseries for fish and invertebrates. *BioScience*, *51*(8), 633-641.
3. Gutiérrez, J., Jones, C., Strayer, D., & Iribarne, O. (2003). Mollusks as ecosystem engineers: the role of shell production in aquatic habitats. Oikos, 101(1), 79–90.
4. La Peyre MK, Serra K, Joyner TA, Humphries A. Assessing shoreline exposure and oyster habitat suitability maximizes potential success for sustainable shoreline protection using restored oyster reefs. Robinson L, ed. *PeerJ*. 2015;3:e1317. doi:10.7717/peerj.1317.
5. Cheng, B., Chang, A., Deck, A., & Ferner, M. (2016). Atmospheric rivers and the mass mortality of wild oysters: insight into an extreme future? Proc. R. Soc. B, 283(1844), 20161462.

Acknowledgements

We would like to sincerely thank the Zacherl Lab and Caitlin Stapp for assisting us in the data collection process and for sharing their data from earlier surveys. We share our thanks with California State University, Fullerton, everyone in the Southern California Ecosystems Research Program, and the Dan Black Challenge to the College of Natural Sciences and Mathematics at California State University Fullerton. Special thanks to Dr. Brian S. Cheng, whose research inspired so many questions for us to try and answer.